SEDIMENT TRANSPORT MODELLING AROUND BRIDGE AT SUNGAI TUI USING 1D QUASI UNSTEADY FLOW HEC-RAS

AMARAN A/L KRISHNAMUTHI

Bachelor of Engineering (Hons) in Civil Engineering

UNIVERSITI MALAYSIA PAHANG

UNIVERSITI MALAYSIA PAHANG

DECLARATION OF THESIS / UNDERGRADUATE PROJECT PAPER AND COPYRIGHT

Author's full name	:**AMRAN A/L KRISHNAMUTHI**
Date of birth	:**31 AUGUST 1991**
Title	:**SEDIMENT TRANSPORT MODELLING AROUND BRIDGE AT SUNGAI TUI USING 1D QUASI UNSTEADY FLOW HEC-RAS**
Academic Session	: **2014/2015**

I declare that this thesis is classified as:

	CONFIDENTIAL	(Contains confidential information under the Official Secret Act 1972)*
	RESTRICTED	(Contains restricted information as specified by the organization where research was done)*
/	**OPEN ACCESS**	I agree that my thesis to be published as online open access (full text)

I acknowledged that University Malaysia Pahang reserves the right as follows:

1. The thesis is the property of University Malaysia Pahang.
2. The Library of University Malaysia Pahang has the right to make copies for the purpose of research only.
3. The Library has the right to make copies of the thesis for academic exchange.

_______________________	_______________________
SIGNATURE	SIGNATURE OF SUPERVISOR
910831055057	DR. BAMBANG WINARTA
(NEW IC NO./PASSPORT NO.)	NAME OF SUPERVISOR
Date: JUNE 2015	Date: JUNE 2015

NOTES: * If the thesis is CONFIDENTIAL or RESTRICTED, please attach with the letter from the organization with period and reasons for confidentiality or restriction

SEDIMENT TRANSPORT MODELLING AROUND BRIDGE AT SUNGAI TUI
USING 1D QUASI UNSTEADY FLOW HEC-RAS

AMARAN A/L KRISHNAMUTHI

Report submitted in fulfillment of the requirements
for the award of the degree of
Bachelor of Engineering (Hons) in Civil Engineering

Faculty of Civil Engineering and Earth Resources
UNIVERSITI MALAYSIA PAHANG

JUNE 2015

SUPERVISOR'S DECLARATION

I hereby declare that I have checked this project report and in my opinion this report is satisfactory in terms of scope and quality for the award of the degree of Bachelor of Engineering (Hons) in Civil Engineering.

Signature	:	
Name of Supervisor	:	DR. BAMBANG WINARTA
Position	:	LECTURER
Date	:	

STUDENT'S DECLARATION

I hereby declare that this report is my own except for the quotations and summaries which have been acknowledged. The report has not been accepted for any degree and is not concurrently submitted for award of other degree.

Signature :

Name : AMARAN A/L KRISHNAMUTHI

ID Number : AA11196

Date :

Dedicated to Dr. Bambang Winarta

ACKNOWLEDGEMENT

Firstly, I would like to express my sincere thanks to my supervisor Dr. Bambang Winarta from Faculty of Civil Engineering and Earth Resources for being instrument in shaping my studies and for being the key figure whose constructive advice contributed immensely towards the completion of this research. Under his supervision, I have learned and gained a valuable knowledge that I cannot found out from the books. He guide and succors me to learn the software of HEC RAS that I did not use before. I manage to learn fast to use the software because every step he taught me, was easily to understand. Once again, thanks for all your guidance and comments that enable me to finish this final year project on schedule.

My gratitude and appreciation also goes to my family, especially my beloved parents Mr Krishnamuthi & Mrs Yogeswari. Thank you so much from the bottom of my heart. They give me warmest supports and advice during my research. They also aid me in term of financial. Besides that, I hereby would also like to thank all of my friends for their support and encouragement during these four years of studying in the university. To my other precious friends as well, you guys have left a mark of happiness and memories in my heart. This campus life would never be the same without your presence.

Last but not least, I have furthermore to acknowledge to lab assistant of geotechnical lab and hydraulic and hydrology lectures for guiding me to conduct experiment for carry out my research. The Faculty of Civil Engineering and Earth Resources had given me the support and approval for the project.

ABSTRACT

Sungai Tui is located in the state of Pahang where huge amount of rainfall during monsoon season subjected to sediment transport process. The river responses by increased or decreased sediment carrying capacity, changing in channel cross section, erosion and deposition along the channel, which impact on river bank stability over a period of time. The research is to model sediment transport around bridge at Sungai Tui by using one dimensional (1D) quasi unsteady flow Hydrologic Engineering Centers River Analysis System (HEC RAS). There is few data required such as catchment area, precipitation data, geometric data and sediment data. The analysis is done using various method of transport function found in HEC RAS. For 5 years analysis of sediment transport, maximum erosion and deposition occurs at the depth 0.49m and 0.64m using Ackers-White; 0.50m and 0.76m using England-Hansen; 0.50m and 1.18m using Laursen; 0.50m and 1.12m using Meyer Peter Muller; 0.49m and 0.48m using Toffaleti; 0.50m and 0.76m using Yang and 0.50m and 1.18m using Wilcock. Erosion and deposition of sediment along the channel is not similar using various methods of transport function. In conclusion, sediment pattern can be predicted and analyzed using several methods in HEC-RAS software.

ABSTRAK

Kajian ini adalah untuk memodelkan pengangkutan sedimen di sekitar jambatan di Sungai Tui dengan menggunakan 1D aliran tak mantap kuasi HEC RAS. Sungai Tui terletak di negeri Pahang di mana sejumlah besar hujan semasa musim tengkujuh tertakluk kepada proses pengerakkan sedimen. Maklum balas sungai dengan ditambah atau dikurangkan sedimen keupayaan membawa, berubah dalam seksyen lintas channel, hakisan dan pemendapan di sepanjang saluran, yang memberi kesan kepada kestabilan bank dalam tempoh masa. Terdapat beberapa data yang diperlukan seperti kawasan tadahan, data pemendakan, geometri data dan data sedimen. Analisis dilakukan dengan menggunakan pelbagai fungsi pengangkutan sedimen terdapat di HEC RAS. Untuk analisis 5 tahun pengangkutan enapan maksimum hakisan dan pemendapan berlaku pada kedalaman 0.49 m dan 0.64 m yang menggunakan Ackers-White; 0.50 m dan 0.76 m yang menggunakan England-Hansen; 0.50 m dan 1.18 m yang menggunakan Laursen; 0.50 m dan 1.12 m yang menggunakan Meyer Peter Muller; 0.49 m dan 0.48 m yang menggunakan Toffaleti; 0.50 m dan 0.76 m Yang menggunakan dan 0.50 m dan 1.18 m menggunakan Wilcock. Hakisan dan pemendapan sedimen di sepanjang sungai tersebut adalah tidak serupa dengan menggunakan pelbagai fungsi pengangkutan sedimen.

TABLE OF CONTENT

LIST OF TABLES

LIST OF FIGURES

LIST OF SYMBOLS

π	Pie
A	Cross section area
Q	Discharge
q	Unit discharge of lateral flow
R	Hydraulic radius
P	Wetted perimeter
W	Top width
h	Mean flow depth
V	Velocity
i	Rainfall intensity
i_b	Infiltration rate
S	Channel slope
S_f	Slope of energy gradient
W_t	Fall velocity
D	Sphere diameter
ρ_s	Density
ρ	Density
g	Gravitational Constant
N	Kinematic viscosity of water
C_a	Concentration
$C^{'}$	Sediment concentration
z	Distance
w_a/KU_o	Rouse number
β	Ratio of diffusion coefficient for sediment over diffusion coefficient for momentum (eddy viscosity)
U_*	Shear velocity
K	Constant
W	Settling velocity
X	Sediment concentration
s	Specific gravity of sediments
d_s	Mean particle diameter

D	Effective depth
V	Average channel velocity
n	Transition exponent depending on sediment size
C	Coefficient
F_{gr}	Sediment mobility parameter
A	Critical sediment mobility parameter.
g_s	Unit sediment transport rate
γ	Unit weight of water
γ_s	Unit weight of solid particles
τ_0	Bed level shear stress
d_{50}	Particle size of which 50% is smaller.
C_m	Sediment discharge concentration, in weight/volume
d_s	Mean particle diameter
τ_c	Critical bed shear stress
k_r	Roughness coefficient
k_r'	Roughness coefficient based on grains,
g	Acceleration of gravity
d_m	Median particle diameter
R	Hydraulic radius
S	Energy gradient
g_{ssL}	Suspended sediment transport in the lower zone
g_{ssM}	Suspended sediment transport in the middle zone
g_{ssU}	Suspended sediment transport in the upper zone
g_{sb}	Bed load sediment transport
g_s	Total sediment transport
M	Sediment concentration parameter
CL	Sediment concentration in the lower zone
z	Exponent describing the relationship between the sediment hydraulic characteristics
n_v	Temperature exponent
C_t	Total sediment concentration

LIST OF ABBREVIATIONS

HEC RAS	Hydrologic Engineering Centers River Analysis System
HEC HMS	Hydrologic Engineering Centers Hydrologic Modeling System
USACE	US Army Corps of Engineers

CHAPTER 1

INTRODUCTION

1.1 RESEARCH BACKGROUND

Malaysia has seen many changes in term of rapid urbanization. This development has accelerated effect on the river catchment areas will cause massive increase in the surface runoff and resulting in higher sediment transport. Sediment transport will be defined as the solid particles such as soil and rock that has been displaced passing each cross section for a specified period of time. Sediment transport is serious dangerous lead to damage the hydraulic structures along the river. When this phenomenon happens, it will not only affect river morphology but also decrease the channel capacity to convey the flood water to downstream and cause instability in the river channel.

Sediment in transport affects the quality of water and its suitability for human consumption or use in various enterprises. Sediment deposited in stream channels reduced the flood-carrying capacity, resulting in more frequent overflow and greater floodwater damage to adjacent properties. The deposition of sediment in irrigation and drainage canals, in navigation channels and floodways in reservoirs and harbors, on streets and highways and in building not only creates a nuisances but also inflicts a high public cost in maintenance removal or in reduced services (Bennett, 1939; Brune, 1958).

The phenomena of sediment transport occurred in rapid development in urban area. The emerging of urban area creates more impervious area. In addition, the amount of impermeable areas will increase for many purpose of landuse (Husan, 1991). The shifting from forest and open space areas to the commercial and industrial area caused substantial changes to the local ecosystem.

Sungai Tui is located in the state of Pahang where huge amount of rainfall during monsoon season subjected to sediment transport process. The river responses by increased or decreased sediment carrying capacity, changing in channel cross section, erosion and deposition along the channel, which impact on bank stability over a period of time. Monitoring and computing the sediment transport is necessary. The research is to model sediment transport around bridge at Sungai Tui by using 1D quasi unsteady flow HEC RAS. Modelling of sediment transport stimulate the sediment pattern around the bridge by using HEC RAS.

1.2 PROBLEM STATEMENT

Movement of sediment in suspension from upstream to downstream may cause several problems. The sediment transport as bed load rolling or sliding along the bed depends on the particle, size, shape, and specific gravity respect to velocity and turbulence. Cobbles move with high velocity and turbulence while silt particles move in low-gradient, low-velocity channels as muddy stream. Muddy stream increase the turbidity leads to decreases the growth of microscopic organisms that feed the fish. The study indicated people concern to fish in muddy stream because the effect of suspended sediment on the size, population and species of fish in a stream (Ellis, 1936). Huge amount sediment transport in river leads to stream morphology of the channel. The flood carrying capacity of the river channel is reduced by high level of sedimentation. This result in greater flood occurs.

1.3 OBJECTIVE OF RESEARCH

The main objective of this research can be outlined as follow:

i. to analysis the pattern of discharge (Rainfall Runoff Relationship).
ii. to stimulate and analysis the pattern of sediment transport around bridge at Sungai Tui, Pahang

1.4 SCOPE OF RESEARCH

The scope of study includes simulating the river using HEC RAS software using gathered data from local authorities. This study involved in the catchment area of Sungai Tui. In this study, a river network was established using the Google satellite images data and the analysis were carried out using river modelling and simulation. The river simulation was carried after all the data were inserted and the networks were created. The river flow from upstream to downstream was marked in the model.

1.5 EXPECTED OUTCOME

This research paper produces a pattern of sediment transport at Sungai Tui, Kuala Lipis, Pahang. Erosion and deposition can be evaluated form the analysis by using HEC RAS for one year, three years, five years and ten years. Sedimentation problem can be solved by increasing cross section of the river. Thus it decreases the flow rate of the river. Apart from that, defense structures such as reservoir, leeves, or weirs can be built to reduce the sediment transport to the downstream.

1.6 SIGNIFICANCE OF THE PROPOSED STUDY

River modelling is the best option to study the behaviors of and what are the influenced factors. By creating the river model based on the actual data and GIS image, the true phenomenon of what is really happened can be understood. The limitation of human activities along the river area could be established after a river simulating was conducted and the hazard risk map was produced. Through this study, the effect of massive water flow around the bridge to the sediment transport occurrences and behaviors could be determined. Thus, for the future, the appropriate early solution could be implemented for massive discharge.

This study is also expected to be able to help the responsible agencies and authorities to river and river basin management to apply more efficient approach for the purpose of analyzing and producing the best design practice in overcoming the sedimentation problems.

CHAPTER 2

LITERATURE REVIEW

2.1 OPEN CHANNEL HYDRAULIC

The learning of the physics of fluids flow in conveyances in which the following fluids forms a free surface and is driven by gravity. There are two types of open channel, natural open channel (river, creek) and artificial open channel (human construction; canals and flumes). The forms of flow in open channel are categorized with respect to time, space, viscosity, density and gravity.

2.1.1 Unsteady Flow in River

The depth varies with both time and space is unsteady flow involves the solution of the energy momentum and friction equations with time. It can be analysed as gradually varied steady flow because the flow is sufficiently close to steady flow.

2.1.2 One Dimensional River Continuity Equation

The figure 2.1 below defines a river reach with cross section area, A, top width W, wetted perimeter P, hydraulic radius $R_h = A/P$, and mean flow depth $h = A/W$. Product of the area A and mean flow velocity V, produce the total discharge Q; the unit discharge of the lateral flow is q_l. The rainfall intensity is i, and the infiltration rate through the wetted perimeter is i_b. The net volumetric flux leaving the control volume is $(\partial Q/\partial x)$ dx + $i_b P$ dx. The net volumetric flux entering the control volume is q_l dx + iW dx. The difference between entering and leaving volumetric fluxes corresponds to volumetric storage ∂A dx = $\partial(Wh)$dx per unit time ∂t .

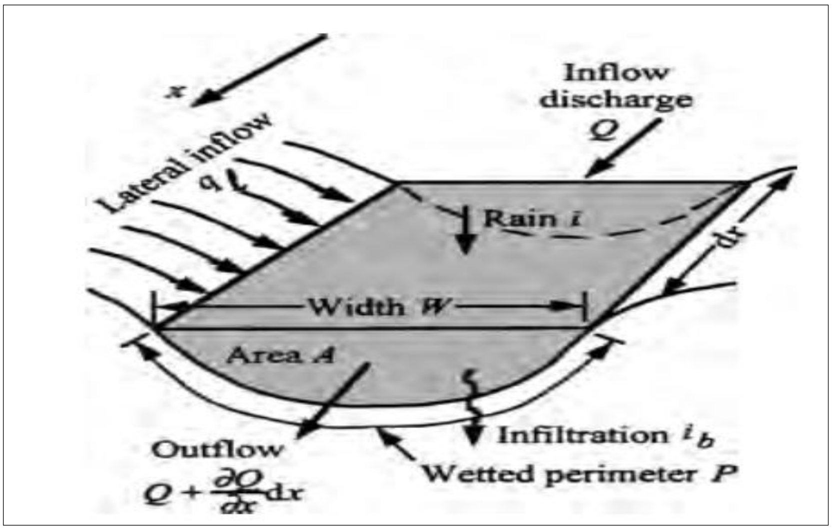

Figure 2.1: Continuity of river reach

Sources: Julien P.Y. (2002)

After dividing by dx, we easily demonstrate that

$$\frac{\partial A}{\partial t} + \frac{\partial Q}{\partial x} + i_b - iW - q_l = 0 \tag{2.1}$$

where i_b is the rate of infiltration through the wetted perimeter P, i is the rainfall intensity through the reach-averaged river width W, A is the reach-averaged cross-sectional area, and q is the unit discharge of lateral inflow. For an impervious channel (i_b=0) without rainfall (i =0) and without lateral inflow (q_l = 0), the1D equation of continuity simply reduces to

$$\frac{\partial A}{\partial t} + \frac{\partial Q}{\partial x} = 0 \tag{2.2}$$

This simple differential equation that expresses conservation of mass is widely used in the analysis of floodwave propagation.

2.1.3 One Dimensional Momentum of River

However, for most practical purposes, the spatial variations in lateral and transverse directions can be neglected and the flow in a river system can be approximated as a one-dimensional process along the longitudinal direction (i.e., in the direction of flow). The Saint Venant equations that were derived in the early 1870s by Barre de Saint-Venant, may be obtained through the application of control volume theory to a differential element of a river reach. The Navier-Stokes equations can be simplified for one-dimensional flow. Assumption made in Saint Venant equations as:

a) The flow is one-dimensional. The water depth and flow velocity vary only in the direction of flow. Therefore, the flow velocity is constant and the water surface is horizontal across velocity is constant and the water surface is horizontal across any section perpendicular to the direction of flow.

b) The flow is assumed to vary gradually along the channel so that the hydrostatic pressure distribution prevails and vertical accelerations can be neglected. The channel bottom slope is small and the channel bed is stable such that there is no change in bed elevations in time. The fluid is incompressible and of constant density throughout the flow.

c) The Manning and Chezy equations, which are used in the definition of channel resistance factor in steady, uniform flow conditions, are also used to describe the resistance to flow in unsteady, non-uniform flow applications.

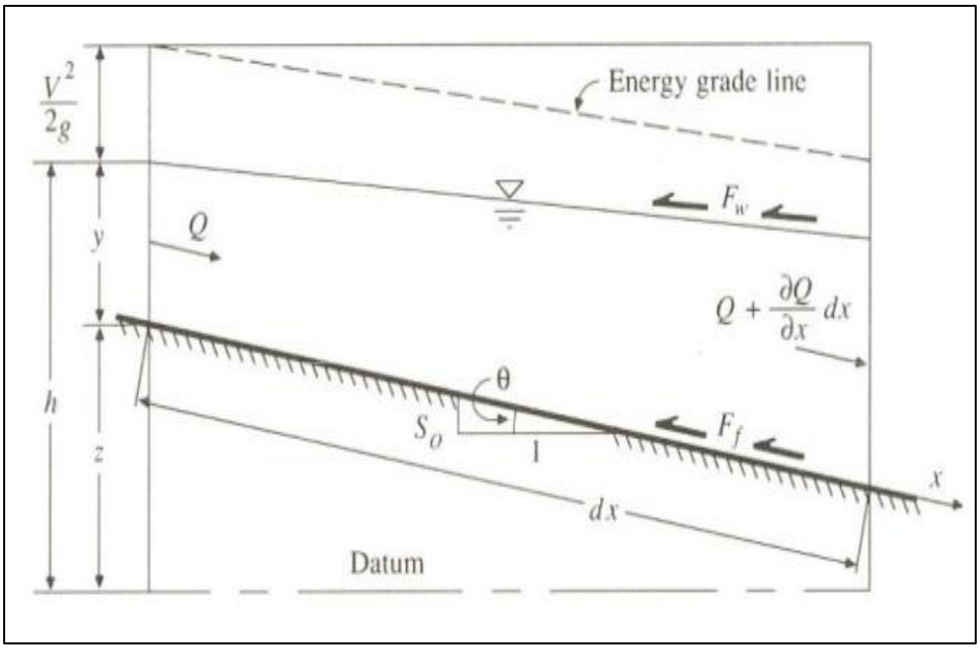

Figure 2.2: Cross section view

Sources: Julien P.Y. (2002)

These equations are the governing equations of one dimensional unsteady flow in open channels and were originally developed by the French scientist Barre de Saint-Venant in 1872.

$$\frac{\partial Q}{\partial t}+\frac{\partial(\beta Q^2)}{\partial x}+gA\left(\frac{\partial h}{\partial x}+S_f+S_e\right)-\beta qv_x+W_fB=0 \qquad (2.3)$$

2.2 SEDIMENT

Sediment is hard or loose material found mainly on the bottom of the river. There are many forms and sizes of sediment. It transported by fluid flow and which eventually is deposited as a layer of solid particles on the bed. The early studies on sediment transport in rigid bed were research by (Craven, 1953; Valentine, 1955; Lauren, 1956). In early stage of research, initial motion on sediments was studies and transporting capacity of the flow was determined for the limit of deposition.

2.3.1 Sediment Transport

No sediment was moved at very low velocities but sediment will transport along the bed at some higher velocity. Motions of sediment in different modes which exist in a stream are defined as follow. Individual grain on the channel bed will roll and slide intermittently along the streambed in the direction of the flow. The sediment so moved is defined as the contact load of the stream. Some grain may also move above the bed surface by saltation. Movement in this mode is describe as saltation load of the stream that occurs when one grain, causing it to jump upward and the fall back toward the bed. Some of the grain transported as suspension if the flow velocity is increasing and the jumps executed by the grain will occur more frequently.

These rolling, sliding, suspension and saltation motions move sediment in a streambed and characterize the transport as bed load. The weight of the sediment related to flow velocity in a stream. In stream channel the transport of sediment as the bed load has been widely studied and a number of empirical equations have been proposed (Einstein, 1942; Meyer-Peter and Muller, 1948; Van Rijn, 1984; Ackers and White et al, 1978).

Motion of sediment in suspension by turbulent eddies are mostly finer-grained. Suspended load is the particles transport within the water column call. If the turbulent is present, there may be continues exchange of sediment between the bed loads of the river. Part of the suspended load may be colloidal clays, which remain in suspension for a very long period of time, depending on the type of clay and water chemistry.

Finest sediment particles in transport are wash load. An inflow of fine sediment in suspension which remain in suspension describe as wash load. The concentration of wash load in suspension is fundamentally independent of hydraulic condition in the stream. Thus, it cannot be calculated using hydraulic parameters such as velocity or discharge. The concentration of wash load is usually a function of supply. As the watershed and banks can transport, the stream can take as much wash load. Figure 2.3 shows various loads within a stream and motion of sediment transport. Figure 2.4 shows sediment transport classification.

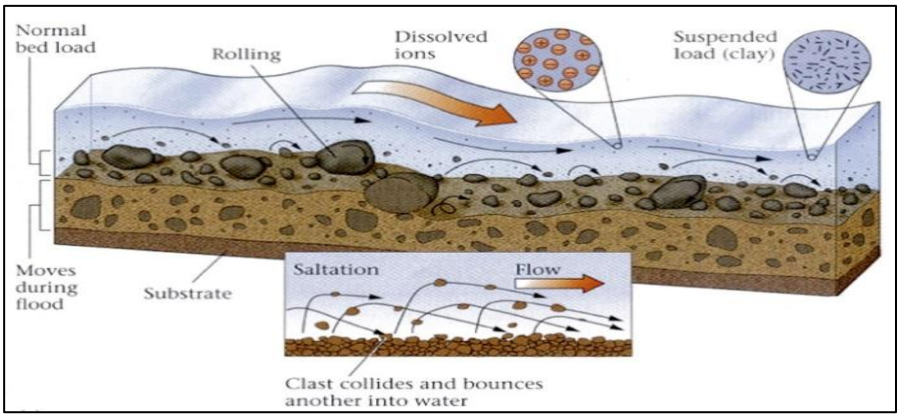

Figure 2.3: Various loads within a stream

Sources: Jansen et al. (1979)

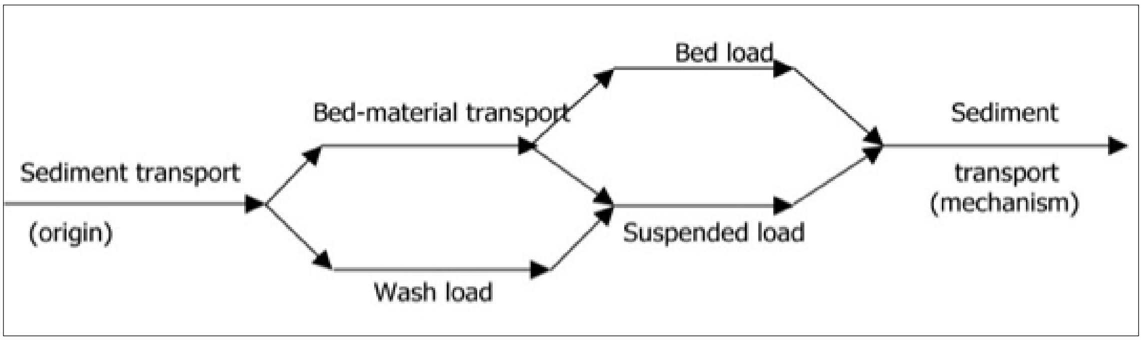

Figure 2.4: Sediment transport classification

Sources: Jansen et al. (1979)

2.3.2 Cohesive and Non-cohesive Sediment

Cohesive and non-cohesive sediment have differences in the natural characteristic. The major discrepancies between suspended cohesive sediment and suspended non cohesive sediment depend on calculation of the settling velocity or fall velocity of sediment, the interchange across the sediment water interface and bed compaction consideration (Van Rijn, 1984). Particles size of cohesive sediment that are smaller than 62µm. In the case, the effect of the flocculation makes settling velocity a function of sediment concentration (Van Leussen, 1994).

Cohesive sediment is the clay-sized materials that are composed, which have strong inner particles forces due to their surface ionic charges. The behavior of sediment dominant by inter particles forces. Its surface area per unit volume (i.e. specific surface area) increases when particles size decrease. There is no clear boundary between cohesive sediment and non-cohesive sediment. The definition is usually site specific. In overall finer sized grains are more cohesive. Sediment sizes smaller than 2 µm (clay) are usually considered cohesive sediment. Silt (2µm-60µm) is well-thought-out to be between cohesive and non-cohesive sediment. The cohesive properties of silt are predominantly due to the presence of clay. Coarse non-cohesive sediment is defined by sediment of size larger than 60 µm. Hence in engineering practice, silt and clay well known be cohesive sediment.

Cohesive sediment contains of organic minerals and inorganic minerals (Hayter, 1983). The organic material is present as animal detritus and plant. There are two types of inorganic minerals such as clay mineral (e.g. illite, kaolinite, montmorrillonite, silica) and non-clay minerals (e.g quartz, mica, and carbonates, among others). Sediment especially cohesive sediment is associated to water quality in stream. Sediment concentration decrease the quality of the water in a stream makes pollutant. In addition, chemicals and wastes are adsorbed to the sediments, are sometimes a water quality concern. The increase in turbidity causes the sunlight evasion to penetrate and decrease the food availability, thus affecting aquatic life. Therefore from the environmental point of view sediment transport is important because there is a link between the presence of sediment and pollutant concentrations (Ashley et al,1991).

2.3.3 Properties of sediment

The discipline of sediment transport interrelated between flowing water and sediment. The study of sediment transport is essential for understanding of the physical properties of water and sediment or sediment is its size. Shape and roundness are vital to the diameter of the grain particles. Shapes define as form of particle whereas roundness defines as the sharpness or radius of its curvature of its edges. For example, a flat particle have a smaller fall velocity than a sphere, but hard for bed load to transport.

Sediment in a stream is naturally occurring material of many different sizes and shapes. The particle size distribution is usually represented by a plot weight percentage of the total sample which is smaller than a given size plotted as function of the particle size. The typical sediment size d_{50} is meant by the sediment size for which 50% by weight of the material is finer. D_{50} is generally used as the characteristic grain size. Due to environmental conditions, the size distribution of cohesive sediment (e.g. clay, silt) may vary to which the sediments have been exposed and also the measures that are used to determine their size distribution. Sediment are classify into two categories: cohesive sediment (e.g. clay and silt) and non-cohesive sediment (e.g. sand, gravel, cobbles and boulders). A typical sediment size classification is shown in table 2.2.

Table 2.1: Sediment size classification

	Class Name	Size Range (mm)
Clay	Very fine clay	0.00024-0.0005
	Fine clay	0.0005-0.0010
	Medium clay	0.0010-0.0020
	Coarse clay	0.0020-0.004
Silt	Very fine silt	0.004-0.008
	Fine silt	0.008-0.016
	Medium silt	0.016-0.031
	Coarse silt	0.031-0.062
Sand	Very fine sand	0.062-0.125
	Fine sand	0.125-0.250
	Medium sand	0.250-0.500
	Coarse sand	0.500-1.000
	Very coarse sand	1.000-2.000

Sources: Vanoni (1977)

Table 2.1: Continue

	Class Name	Size Range (mm)
Gravel	Very fine gravel	2-4
	Fine gravel	4-8
	Medium gravel	8-16
	Coarse gravel	16-32
	Very fine gravel	32-64
Cobbles	Small cobbles	64-128
	Large cobbles	128-256
Boulders	Medium boulders	256-512
	Coarse boulders	512-1024
	Very large boulders	1024-2048
	Small cobbles	2048-4096

2.3.4 Fall Velocity

Fall velocity is the velocity at which a sediment particle falls through a fluid. The velocity reflects the shape, particle size and weight as well as the fluid characteristic. In a quiescent fluid (water), we consider a sphere of diameter D that is released at zero velocity. Fluid resistance reduces the acceleration to equilibrium as the fall velocity ω increases. At equilibrium, the gravity forces is in balance with the drag force and terminal velocity, W_t exist.

$$w_t = \left(\frac{D^2 g}{18v}\right)\left(\frac{\rho_s}{\rho} - 1\right) \tag{2.4}$$

Sediment particles are somewhat smaller than spherical, and for a given diameter, based on a sieve analysis; they usually have a fall velocity a little smaller than that of a sphere of the same diameter. In general, stroke lay is applicable to gravity particles in the silt and clay-size range falling in fluid. They are obviously referred to as wash load because these fine materials tend to wash on through the system. Form drag and surface drag are two types of drag.

2.3.5 Bed Forms and Flow Resistance

Free surface flow over erodible sand beds produces a range of different bed forms and bed configuration. The type and dimension of a bed form depends on the properties of the flow, fluid and bed material. Table 2.2 shows summary description of bed forms arranged in increasing order of sediment transport rate. Because there is a hard connection among the flow resistance, the bed configuration and the rate of the sediment, it is vital to know the circumstance under which different bed forms exist.

Table 2.2: Bed form classification

Bed form	Dimensions	Shape	Behavior and occurrence
Ripples	Wavelength less than approx. 1ft;height less than approx. 0.1ft	Roughly triangular in profile, with gentle, slightly convex upstream slopes and downstream slopes nearly equal to the angle of the repose. Generally short-creasted and three-dimensional	Move downstream with velocity much less than that of the flow. Generally do not occur in sediments coarser than about 0.6mm
Bars	Lengths comparable to the channel width height comparable to mean flow depth	Profile similar to ripples plan form variable	Four types of bats are distinguished: 1. point 2. alternating 3. transverse 4. tributary. Ripples may occur on upstream slopes

Sources: Vanoni (1977)

Table 2.2: Continue

Bed form	Dimensions	Shape	Behavior and occurrence
Dunes	Wavelength and height greater than ripples but less than bars	Similar to ripples	Upstream slopes of dunes may be covered with ripples. Dunes migrate downstream in manner similar to ripples.
Transition	Vary widely	Vary widely	A configuration consisting of a heterogeneous arry of bed forms, primarily low amplitude ripples and dunes interspersed with flat regions
Flat bed	-	-	A bed surface devoid of bed forms. May not occur for some ranges of depth and sand size
Antidumes	Wave length = $2\pi v^2/g$ (approx.)[a] Height depends on depth and velocity of flow	Nearly sinusoidal in profile. Crest length comparable to wavelength	In phase with and strongly interact with gravity water surface waves. May move upstream, downstream or remain stationary depending on properties of flow and sediment.

Figure 2.5 shows bed form charts for flow depths up to 10 ft (3 m) and also between 100 µm and 600 µm from (Vanoni, 1974). Bed form is typically classified into a lower regime for subcritical flow, and an upper regime for supercritical flow, with a transition zone close to critical flow.

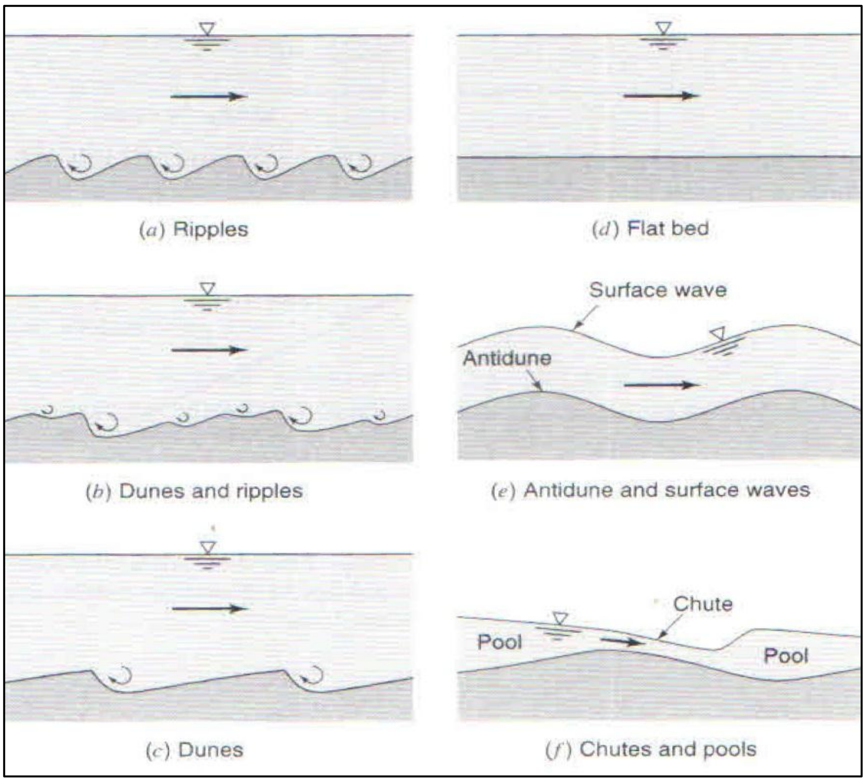

Figure 2.5: Bed form charts

Sources: Vanoni (1974)

Factors that affect bed form and resistance to flow include fine material concentration, water depth, fluid density, seepage force, slope, bed-material size, channel cross-sectional shape, bed-material gradation, fall velocity of sediment particles and others mention to (Simons and Senturk, 1977; and Yang, 1996) for further discussion.

2.3.6 Sediment Transport Function

Table 2.2 shows summary description of sediment transport function used in to analyzed sediment transport analysis.

Table 2.3: Sediment transport function

Function name	Type	Sediment size range (mm)	Develop form	Comments
Ackers-White	Total Load	0.04-2.5	Flume data	Provides good description of movement for lightweight sediments in laboratory flumes and natural rivers
Yang	Total load	0.015-1.71	Stream data	The function is effective for sediments with specific gravity of 2.65. Yang's sand formula is adaptable for sand-bed laboratory flumes and natural rivers-wash load excluded. Yang's gravel formula is for bed material between 2 and 10 mm.
Meyer-Peter Muller	Bed load	0.40-30	Flume data	Not valid for flows with appreciable suspended loads. The function was calibrated for coarse sands and gravels. It is recommended for rivers when the bed material is coarser than 5mm. Depth range is from 1 to 1.2 m.

Sources: Vanoni (1977)

Table 2.3: Continue

Function name	Type	Sediment size range (mm)	Develop form	Comments
Toffaleti	Total load	0.062-16	Stream data	The bed load portion may be calculated by a load function (for example, Schoklitsch, or Meyer-Peter and Muller). It should not be used for lightweight and coarser material but is adaptable for large sand-bed rivers with specific gravity of 2.65.
Laursen	Total load	0.01-4.08	Flume data	Intended to be applied only to natural sediments with specific gravity of 2.65. It is adaptable for shallow rivers with fine sand and coarse silt.
Engelund-Hansen	Total load	Sizes in excess of 0.15mm	Large Flume data	Appears to satisfactorily predict sediment discharge in sand-bed rivers
Wilcock	Bed load	2-64	Stream data	

2.3.7 Suspended Load Transport

Sediment along a stream bed will move when the flow condition satisfy or at higher shear stress. Bed load transport classify as sediment is rolling, sliding or jumping along the bed. Bed load transport rate of a river is about 5%-25% of suspension. The motion of the sediment when it is surrounded by fluid describe as sediment in suspension. Suspended sediment is defined by the amount of sediment transported by suspension.

Advencive turbulent diffusion and convective causes the movement of suspended matter. The diffusion characterizes the random motion and mixing of sediment through the water depth superimposed to the longitudinal flow motion. When the turbulent mixing length is greater, sediment motion by convection occurs compared with the sediment distribution length scale. The effect of suspended sediment on turbulent flow and the difference between water flow and suspended sediment is now well reorganized the variation of the mean velocity profile in the vertical plane state by (Dyer and Soulsby, 1988; McLean, 1992). Solid particles as analogous to molecules of gas kinetic theory of gas and described them by boltzmam equation in the two phase theory (Wang and Ni, 1991). Combination of kinetic theory and continuum theory, explicit particle velocity distribution function was obtained and a model for sediment concentration profile was developed. Using two phase flow theory similar results were gain by (Zaichik et al, 1997; Hyland et al, 1999; Derevich, 2000; fu et al, 2001; Fu and Wang, 2003). These studies have an enhanced understanding of the mechanism of sediment suspension and concentration distribution.

The sediment diffusivity may be assumed to be nearly equal to the turbulent diffusion coefficient (i.e the eddy viscosity). The eddy viscosity is a coefficient of momentum transfer. It expresses the transfer of momentum from points where the momentum per unit volume is high to points where it is lower. Combination of convection and diffusion are one of an alternative approach, thus dealing explicitly with the upward transport of sediment in traveling vortices (Nielsen 1995). The integration of the continuity equation for sediment gives the distribution of sediment gives the distribution of sediment concentration across flow depth:

$$\frac{C'}{C_a} = \left(\frac{h-z}{z} x \ \frac{a}{h-a}\right)^{w_a/KU_*} \tag{2.5}$$

Where Ca is the reference concentration (g/L) at the distance above the bed (m), h is water depth (m) and w_a/KU_* is the Rouse number of supended sediment, which determines the degree of uniformity of suspension). The smaller the Rouse number, the more uniform the suspension is. Equation was develop by Rouse (1937) and it was successful examines with laboratory and field data (e.g Vanoni1946). Figure 2.6 shows Rouse solution for vertical distribution of suspended sediment concentration.

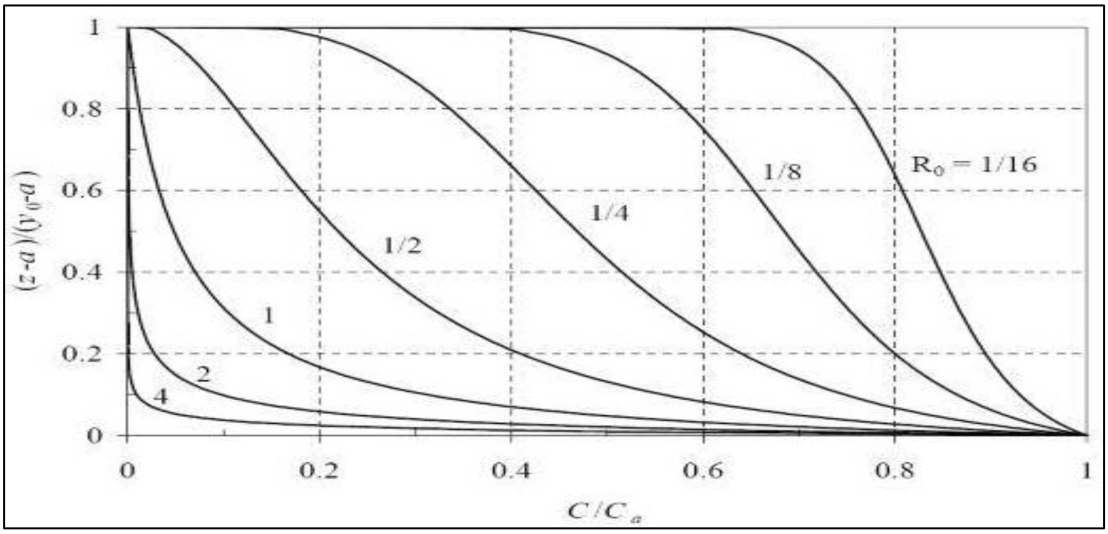

Figure 2.6: Rouse solution for vertical distribution of suspended sediment concentration

Sources: Rouse (1937)

2.3 8 Deposition Process

When the critical shear stress is greater than the bottom shear stress, deposition of sediment occurs. Depositions take place when a stream lack of energy to carry its loads. For bed load materials, deposition occurs when material stop roiling, sliding or jumping. In contrast, deposition occurs when the material settle out of suspension for suspended load. In still water, a particle will settle out a rate dependent on its terminal velocity. (Briggs, 1997) discusses three major processes which lead to deposition sediment:

a) The placement of the sediment in the flow changes, increasing resistance. The lift and drag on a non-spherical sediment will change with placement. The force acting on the sediment will also affect its placement on the bed

b) The capability of the stream decrease. It was meaning that the energy available for transporting sediment decrease. Suspended sands and gravels settle out when stream flow drops, and when a local velocity decreases such in river.

c) The quantity or size of the sediment load suddenly increases. This type of deposition may occur if a stream suddenly receives an influx of sediment from a landslide or collapsing stream bank.

2.3 RIVER MORPHOLOGY

Since then considerable interest has been evinced in changes in drainage pattern and channel changes as can be seen from the works of (Allen, 1965; Leopold et al. 1964; Schumm, 1969; Schumm, 1971; Schumm, 1977). These changes are briefly discussed herein. (Lewin, 1977) classifies channel changes into two categories namely autogenic changes and allogenic changes. Autogenic changes are the ones which are inherent in the river regime and involve avulsion, channel migration, cut-offs and crevassing. Allogenic changes are the ones which occur in response to system changes involving climatic fluctuations and altered sediment load or discharges, as a result of human activity. If a channel is migrating in the valley created by it, some geomorphologists consider such a stream, in regimen. The type of changes that take place in the stream as it debouches from mountains and joins the sea stated by (Newson, 1995). Figure 2.7 indicates that avulsion is more likely to occur when stream is about to enter from steep slope region into the plain with flatter slope. Bank erosion, bar formation and meander shifting occur in the middle reaches, slumping of banks, building of flood plain and channel migration take place in the lower reaches.

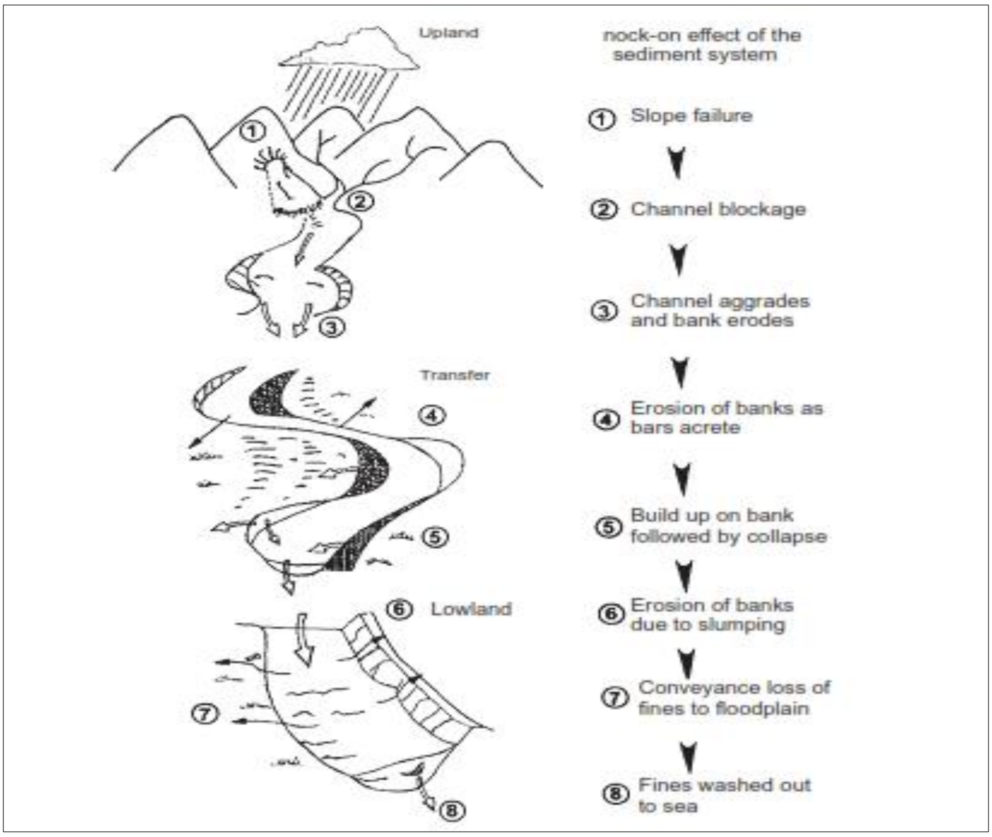

Figure 2.7: Alluvial stream problem problems involving erosion and deposition

Sources: Newson (1995)

2.3.1 Riverbed Degradation

Channel degradation refers to the general lowering of the bed elevation that is due to erosion. In some cases, the bed material is fine and degradation will result in channel incision. In other cases, the material is sufficiently coarse to form an armor layer that prevents further degradation.

Slope adjustments refer to streams that would require either a steeper or a milder slope for reaching equilibrium between incoming and outgoing water and sediment discharges. Stated in simple terms, when the outgoing exceeds the in flowing sediment load, alluvial streams will scour bed material and degrade.

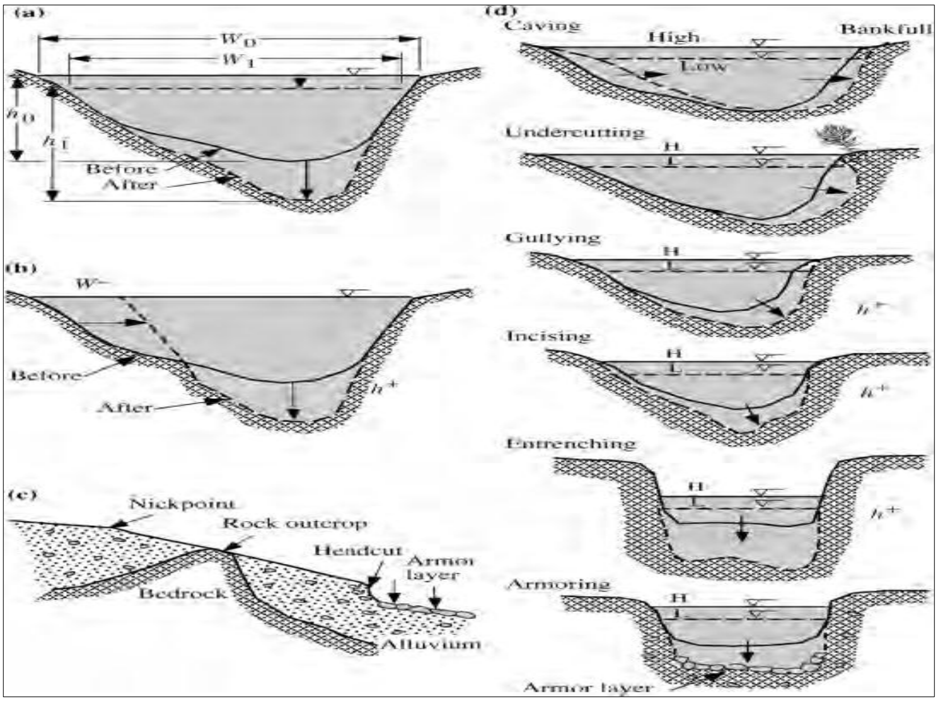

Figure 2.8: Schematic of riverbed degradation

Sources: Newson (1995)

Incised channels tend to be narrow and deep compared with equilibrium conditions. Channel incision will occur until equilibrium condition is reached. Incised channels are typical of upland areas whereby the sediment-transport capacity increases in the downstream direction. Rills are small-scale channels found in upland areas. Gullies are larger-scale features also found in upland areas. Conventionally, rills can be crossed by farm machinery whereas gullies cannot. In rivers, channel incision is found in arroyos and canyons. Arroyos are ephemeral channels in arid areas with flashy hydrographs that carry large sediment loads during short periods of time. Many arroyos dry out in the downstream direction due to infiltration and evaporation. The sediment load eventually deposits on the channel bed downstream of arroyos to form wide-shallow streams. Canyons are usually deeply entrenched in vertical bedrock walls. Incised channels typically are narrower and deeper then equilibrium channels and are characterized by a shortage of sediment.

Channel degradation also causes the banks to become unstable and subject to failure. Gully-like incised channels become very unstable, and bank erosion may become a significant source of sediment to the channel. Incised channels often be found where the stream slope increases in the downstream direction. Knickpoints indicate points with a sudden change in bed slope. Headcuts refer to sudden drops in bed elevation. Headcuts start downstream, and their upstream migration is a characteristic feature of incised channels. Degradation of the main river stem at river confluences causes headcutting and degradation in the tributaries. Figure 2.9 show the headcut propagates upstream from the confluence cause severe stability problems in structures on shallow foundations such as bridges and some grade-control structures. The ensuing gullying in a tributary affects significant bank instabilities and channel widening.

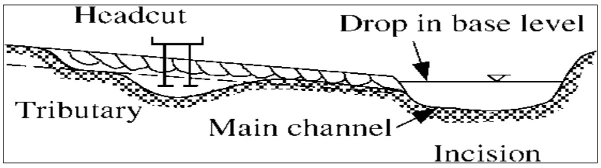

Figure 2.9: Schematic of headcut migration

Sources: Newson (1995)

Armoring of the bed layer refers to coarsening of the bed-material size as a result of degradation of well-graded sediment mixtures. The selective erosion of finer particles of the bed material leaves the coarser fractions of the mixture on the bed to induce coarsening of the bed material. When the applied bed shear stress is sufficiently large to mobilize the larger bed particles, degradation continues; when the applied bed shear stress cannot mobilize the coarse bed particles, an armor layer forms on the bed surface. The armor layer becomes coarser and thicker as the bed degrades until it is sufficiently thick to prevent any further degradation. The armor layer is representative of stable bed conditions and can be mobilized only during large floods. A riverbed is sometimes said to be paved when the armor layer can be mobilized only during exceptional floods. Three conditions need to be satisfied to form armor layers: (1) the stream must be degrading, (2) the bed material must be sufficiently coarse, and (3) there must be a sufficient quantity of coarse bed material.

2.3.2 Riverbed Aggradation

Channel aggradation refers to a gradual bed-elevation increase that is due to bed load sedimentation. When the inflowing sediment discharge exceeds the outgoing sediment capacity, alluvial channels tend to deposit their sediment load throughout the reach. Streams carrying mostly wash load will not change their morphology because the sediment overload will be carried downstream to settle in lakes, reservoirs, or estuaries. Streams carrying most of their sediment load in suspension change their morphology gradually as the excess sediment load settles in the downstream direction. The riverbed material size becomes gradually finer in the downstream direction. From Lane’s relationship, downstream fining is usually accompanied by a downstream decrease in bed slope. On the other hand, streams that carry predominantly bed load material will respond quite rapidly to a change in sediment-transport capacity. A decrease in transport capacity induces direct settling on the bed of alluvial channels.

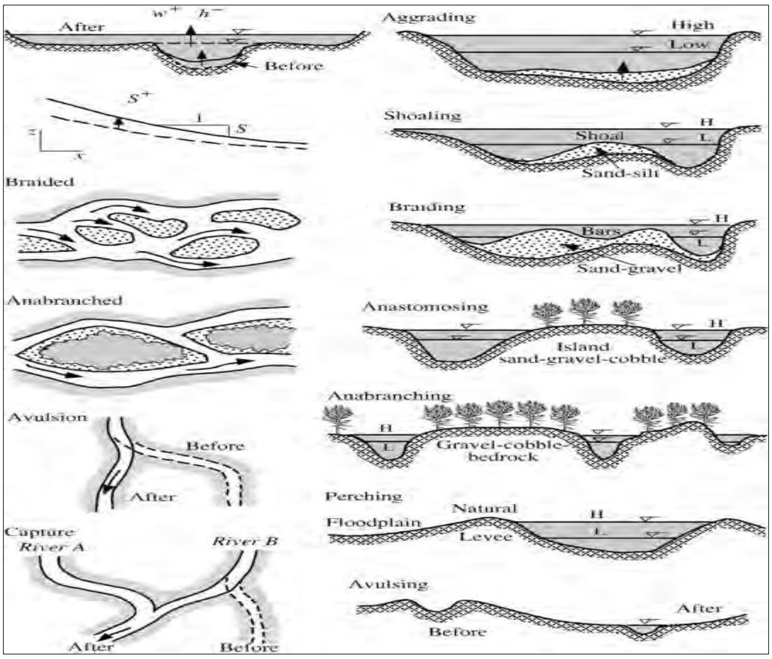

Figure 2.10: Schematic features of riverbed aggradation

Sources: Newson (1995)

2.4 HECRAS

HEC RAS is one-dimensional hydraulic analysis software produced by US Army Corps of Engineers (USACE, 1991). The software consists of four elements for steady flow water surface calculation, unsteady flow stimulation, water quality analysis, and sediment transport stimulation that use hydraulic computation routines and geometric data. Basic water surface profiles can generate using several hydraulic design features. In addition, HEC RAS can predict the changes in channel bed and river profiles from troubles such as flood plain. It is capable to analysis sediment transport.

2.4.1 Quasi Unsteady Flow

River hydraulics should accomplish before run sediment transport in HEC RAS. Many sediment transport models use a hydrodynamic simplification by HEC RAS. A continuous hydrograph with a series of discrete steady flow profiles that divide into shorter blocks of time for sediment transport computations is estimates assumption of the quasi-unsteady flow. HEC-RAS utilizes the three time steps are the flow duration, the computation increment, and the mixing time step for each a subdivision of another.

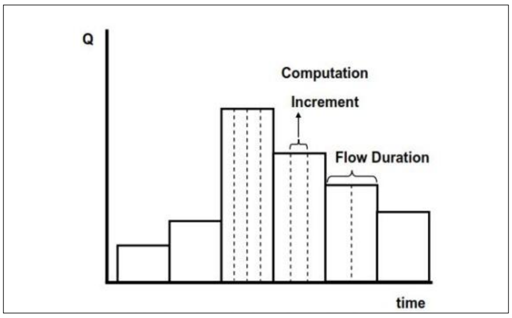

Figure 2.11: A quasi unsteady flow series with time step.

Sources: USACE (1991)

2.4.2 Sediment Continuity

Exner equation known as sediment continuity equation evaluate by the HEC RAS sediment routing routines. Sediment volume in a control volume is equal to the difference between the inflowing and outflowing loads define by the equation. Sediment deficit is satisfied by eroding bed sediments if the capacity is greater than supply whereas sediment surplus causing material to deposit if supply exceeds capacity.

$$(1-\lambda_p)B\frac{\partial\eta}{\partial\tau}=-\frac{\partial Q_s}{\partial x} \tag{2.6}$$

Figure 2.12 shows schematic control volume used by HEC RAS for sedimentation calculation

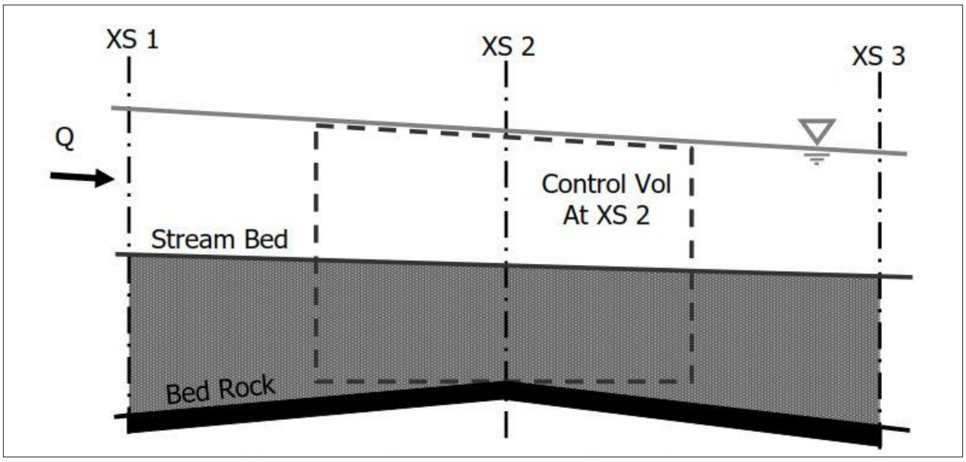

Figure 2.12: Schematic control volume

Sources: USACE (1991)

2.4.3 Compute Transport Capacity

Sediment transport capacity is a function of the amount of sediment that can leave the control volume. HEC RAS divide the 20 grain classes of sediment material range between 0.002mm and 2048mm. HEC RAS uses the geometric mean of the grain class to represent the grain size for each classes.

General equation for Acker-White transport function for single grains size is:

$$X = \frac{C\left(\frac{F_{gr}}{A} - 1\right) s d_s}{D\left(\frac{u_*}{V}\right)^n} \tag{2.7}$$

where X is sediment concentration, in parts per part, s = specific gravity of sediments, d_s = mean particle diameter, D = effective depth, u_* is shear velocity, V is average channel velocity, n is transition exponent depending on sediment size, C is coefficient, F_{gr} is sediment mobility parameter and A is critical sediment mobility parameter.

General equation for England Hansen transport function is:

$$g_s = 0.05\gamma_s V^2 \sqrt{\frac{d_{50}}{g\left(\frac{\gamma_s}{\gamma} - 1\right)}} \left[\frac{\tau_0}{(\gamma_s - \gamma) d_{50}}\right]^{3/2} \tag{2.8}$$

where g_s is unit sediment transport, γ = unit wt of water, γ_s = unit wt of solid particles, V is average channel velocity, τ_0 is bed level shear stress and d_{50} is particle size of which 50% is smaller.

General equation for Laursen transport function for single grains size is:

$$C_m = 0.01\gamma\left(\frac{d_s}{D}\right)^{7/6}\left(\frac{\tau_0{}'}{\tau_c} - 1\right) f\left(\frac{u_*}{\omega}\right) \tag{2.9}$$

where C_m is sediment discharge concentration, in weight/volume, γ is unit weight of water, d_s is mean particle diameter, D is effective depth of flow, τ_0 is bed shear stress due to grain resistance, τ_c is critical bed shear stress and $f\left(\frac{u_*}{\omega}\right)$ is function of the ratio of shear velocity to fall velocity.

General Meyer Peter Muller transport function is:

$$\left(\frac{k_r}{k_r'}\right)^{3/2} \gamma RS = 0.047\,(\gamma_s - \gamma)d_m + 0.25\left(\frac{\gamma}{g}\right)^2 \left(\frac{(\gamma_s - \gamma)}{\gamma_s}\right)^{2/3} g_s^{\,2/3} \qquad (2.10)$$

where g_s is unit sediment transport rate in weight / time / unit width, k_r is roughness coefficient, k_r' is roughness coefficient based on grains, γ is unit weight of water, γ_s is unit weight of the sediment, g is acceleration of gravity, d_m is median particle diameter, R is hydraulic radius and S is energy gradient.

General equation for Toffaleti transport function for single grains size is:

$$g_{ssL} = M\,\frac{\left(\frac{R}{11.24}\right)^{1 + n_v - 0.756z} - (2d_m)^{1 + n_v - 0.756z}}{1 + n_v - 0.756z} \qquad (2.11)$$

$$g_{ssM} = M\,\frac{\left(\frac{R}{11.24}\right)^{0.244z}\left[\left(\frac{R}{2.5}\right)^{1 + n_v - z} - \left(\frac{R}{11.24}\right)^{1 + n_v - z}\right]}{1 + n_v - z} \qquad (2.12)$$

$$g_{ssU} = M\,\frac{\left(\frac{R}{11.24}\right)^{0.244z}\left(\frac{R}{2.5}\right)^{0.5z}\left[\left(\frac{R}{2.5}\right)^{1 + n_v - 1.5z} - \left(\frac{R}{11.24}\right)^{1 + n_v - 1.5z}\right]}{1 + n_v - 1.5z} \qquad (2.13)$$

$$g_{sb} = M\,(2\,d_{\mathrm{m}})^{1 + n_v - 0.756z} \qquad (2.14)$$

$$M = 43.2\,C_L\,(1 + n_v)\,VR^{0.756\,z - n_v} \qquad (2.15)$$

$$g_s = g_{ssL} + g_{ssM} + g_{ssU} + g_{sb} \qquad (2.16)$$

where g_{ssL} is suspended sediment transport in the lower zone, in tons/day/ft, g_{ssM} is suspended sediment transport in the middle zone, in tons/day/ft, g_{ssU} is suspended sediment transport in the upper zone, in tons/day/ft, g_{sb} is bed load sediment transport in tons/day/ft, g_s is total sediment transport in tons/day/ft, *M* is sediment concentration parameter, *CL* is sediment concentration in the lower zone, *R* is hydraulic radius, *dm* is median particle diameter, *z* is exponent describing the relationship between the sediment and hydraulic characteristics and n_v is temperature exponent

General equation for Yang transport function for single grains size is:

For sand $d_m < 2$

$$\log C_t = 5.435 - 0.286 \log\left(\frac{\omega d_m}{v}\right) - 0.457 \log\left(\frac{u_*}{\omega}\right) + \left[1.799 - 0.409 \log\left(\frac{\omega d_m}{v}\right) - 0.314 \log\left(\frac{u_*}{\omega}\right)\right] \log\left(\frac{VS}{\omega} - \frac{V_{cr}S}{\omega}\right) \quad (2.17)$$

For sand $d_m \geq 2$

$$\log C_t = 6.681 - 0.633 \log\left(\frac{\omega d_m}{v}\right) - 4.816 \log\left(\frac{u_*}{\omega}\right) + \left[2.784 - 0.305 \log\left(\frac{\omega d_m}{v}\right) - 0.282 \log\left(\frac{u_*}{\omega}\right)\right] \log\left(\frac{VS}{\omega} - \frac{V_{cr}S}{\omega}\right) \quad (2.18)$$

where C_t is total sediment concentration, ω is particle fall velocity, d_m is median particle diameter, v is kinematic viscosity, u_* is shear velocity and V is average channel velocity.

2.4.4 Bed Changes

Erosion and deposition mass can compute once surplus or deficit is fixed. The mass is added or subtracted from the control volume by changing the cross section station points.

CHAPTER 3

METHODOLOGY

3.1 SITE DESCRIPTION

This research took place in Sungai Tui, Kuala Lipis, Pahang. The length of the stream is about 3.1 km. The estimate terrain elevation above sea level is 75 meters. The shape of the stream is irregular along the river. The estimate width of the stream is approximately m. The entire area for river basin of Sungai Tui is 66.1 km^2. The stream linked with many sub-stream, and connected to the downstream, Sungai Jelai. Figure below shows the river basin of Sungai Tui. On the other hand, my research is mainly focus sediment transport around the 1^{st} bridge along the stream. There are many villages along the stream (e.g Kampung Kuala Tui)

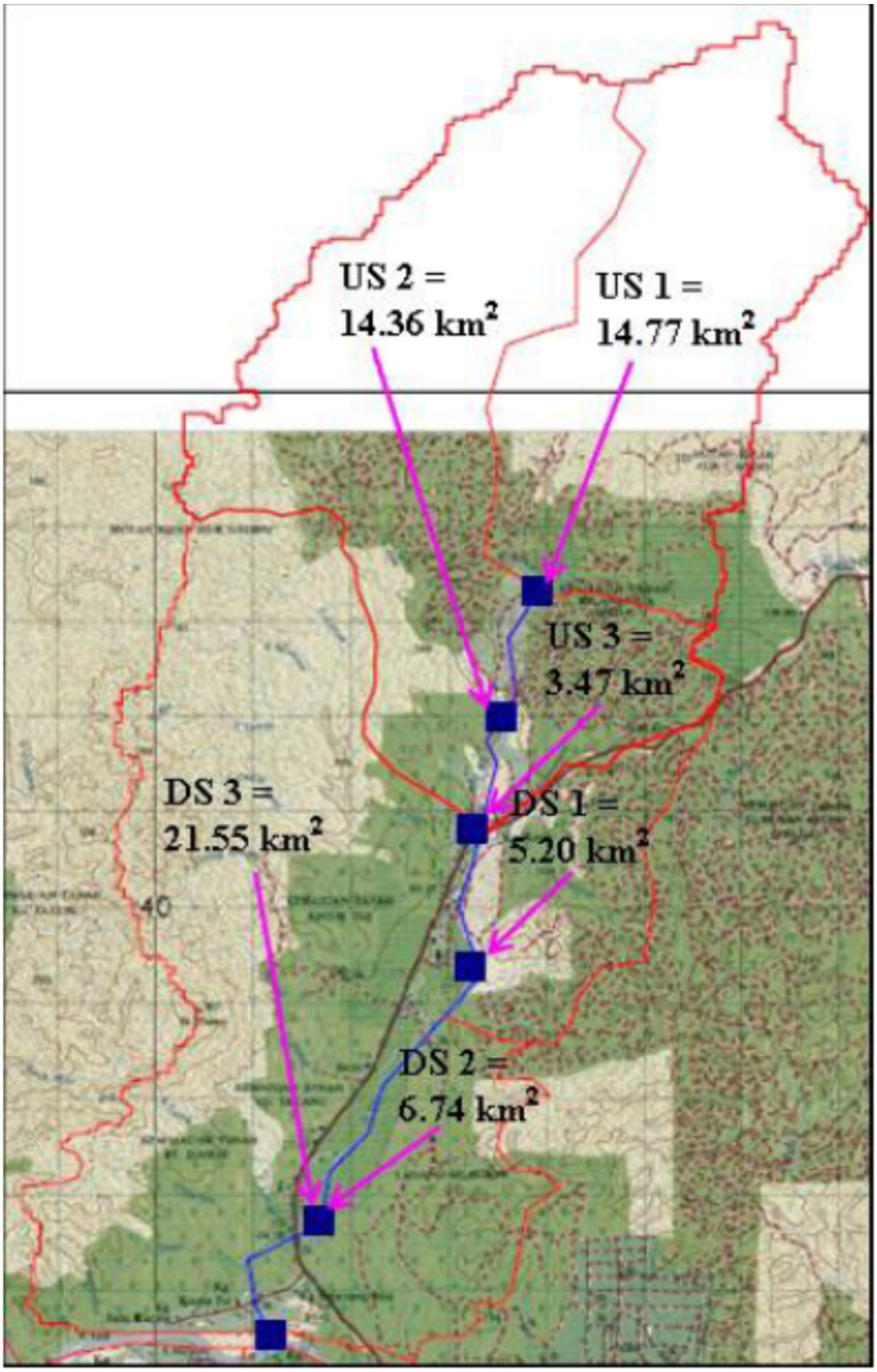

Figure 3.1: River basin of Sungai Tui, Pahang

3.2 PRIMARY DATA ANALYSIS

Primary data is a type of information that is obtained directly from first-hand sources by means of surveys, observation or experimentation. It is data that has not been previously published and is derived from a new or original research study and collected at the source. In this case study, the experimentation of sieve analysis in geotechnical laboratory ump using sediment sample is collected from Sungai Tui are recorded. Sediment is classified into two categories such as cohesive sediment and non-cohesive sediment. Cohesive is a mixture of clay and small amount of silt and sand. It can be describe as mud stream. Non cohesive sediment is boulder, cobble, gravel and sand.

3.3 SECONDARY DATA ANALYSIS

Secondary data is the data taken from the other trusted organization which helps to gather the information for the proposed thesis. To model the sediment transport by using HEC RAS, there is few secondary data required such as discharge rate, catchment area details, geometric bridge data and sediment data. Precipitation data from rainfall stations Bukit Betong and Sek. Keb. Kg. Aur Gading were collected from Department of Irrigation and Drainage. This data used to determine the discharge flow. Topographic map of Sungai Tui collect from Department of Survey And Mapping Malaysia. Basically to model the sediment transport, we required to know initial condition and transport parameters.

3.4 TYPE OF DATA

There are several types data required in modelling of sediment transport around bridge at Sungai Tui, Pahang, by using 1D quasi unsteady flow.

i. Catchment area
ii. Precipitation data
iii. Geometric bridge data
iv. Sediment data

3.5 CASE STUDY

This study gives a better view and illustrates the actual modelling of the sediment transport at around bridge Sungai Tui, Pahang. This is a study to understand the pattern of sediment transport within the river. Moreover, erosion and deposition of sediment can be evaluated from the sediment analysis. Base on the hydrologist, the higher the flow velocity of water, the more capacity of water to transport sediment along the river.

3.6 FLOW CHART OF STUDY

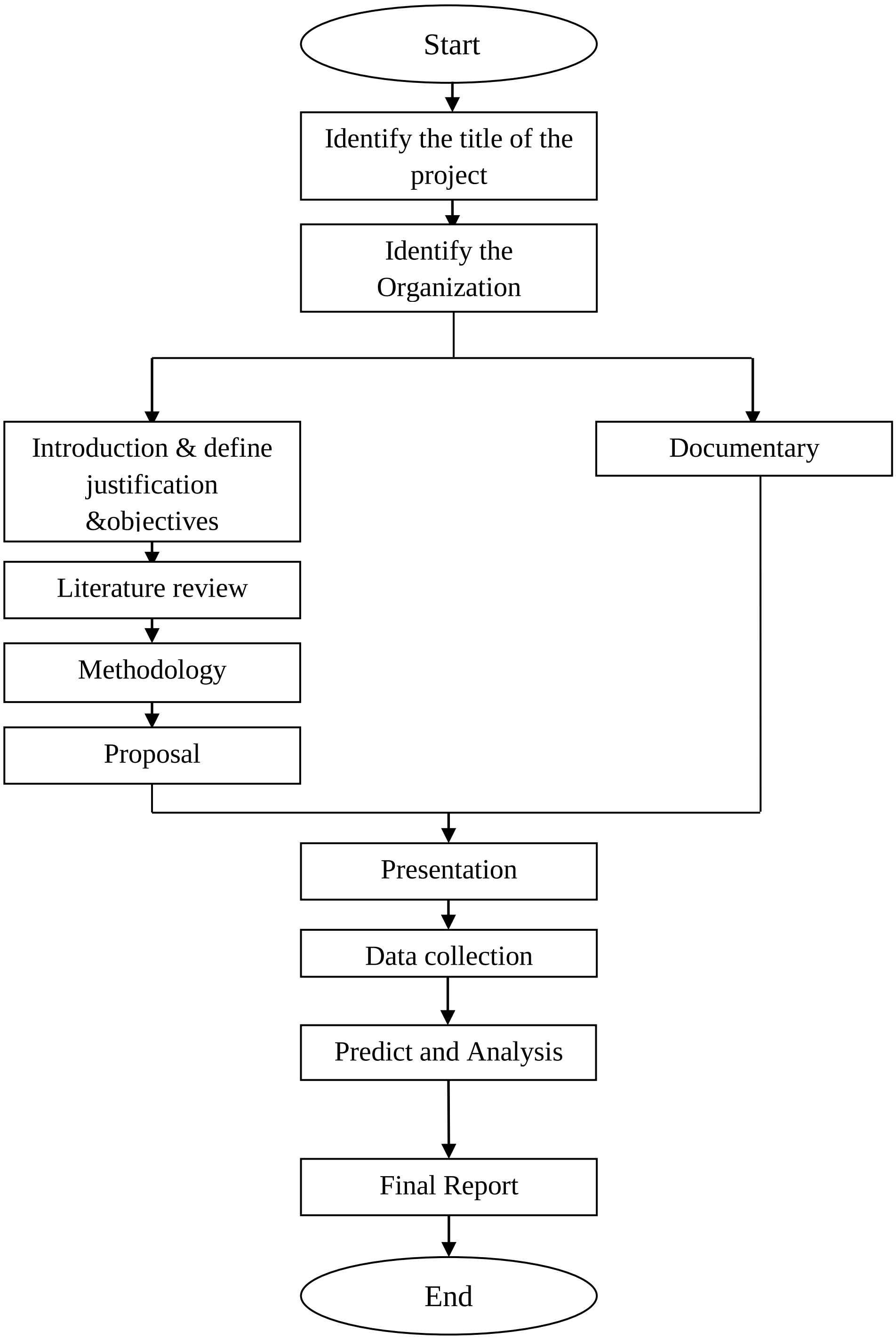

Figure 3.1: Methodology of case study

3.7 FLOW CHART OF SEDIMENT TRANSPORT

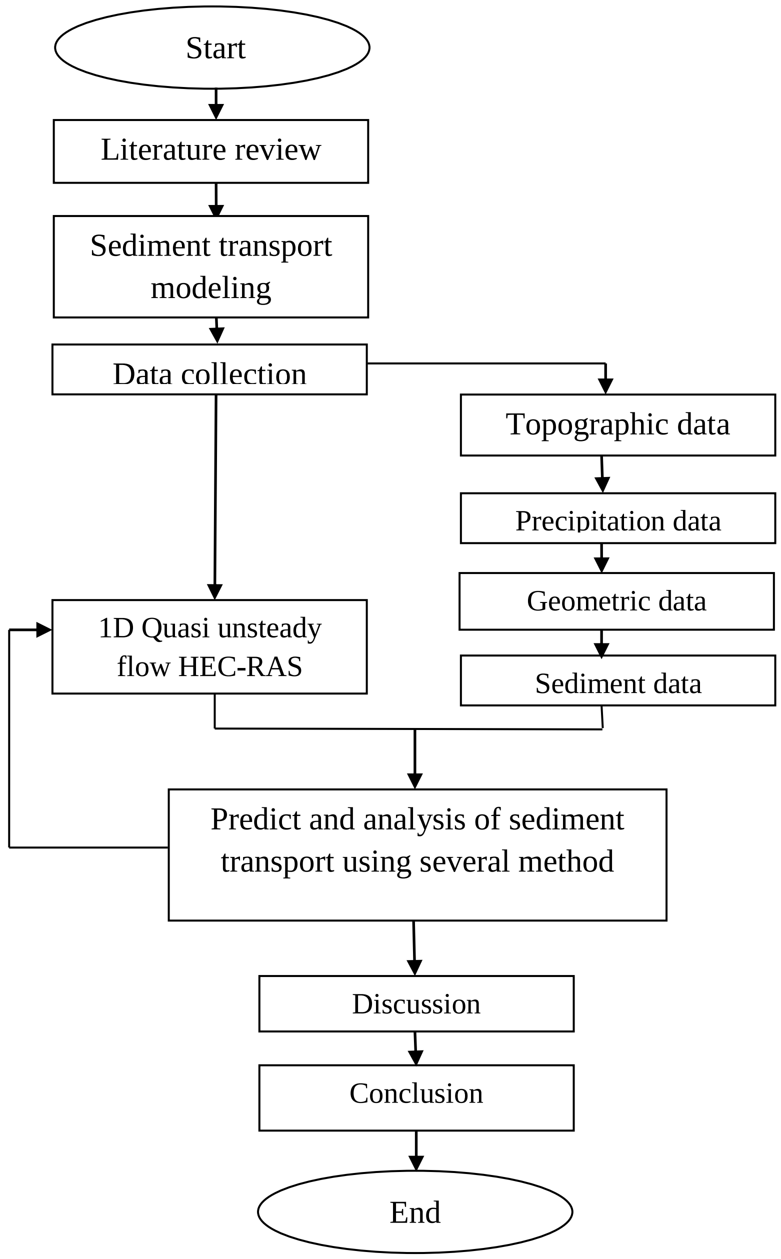

Figure 3.2: Methodology of sediment transport

CHAPTER 4

ANALYSIS AND DISCUSSION

4.1 STREAM FLOW GENERATION

4.1.1 HYDROLOGICAL MODEL CALIBRATION

Since there is no stream flow gauge in Sungai Tui for use in sediment transport analysis, stream flow data is generated by rainfall data using HEC HMS. Time of concentration is used to compute rainfall-runoff parameter in sub catchment.

Calibration of hydrological model is essential and based on one flood event occurred on November 9, 2013. Flood discharge condition due to 127 mm accumulation depth on November 9, 2013 in the confluence of Sungai Tui and Sungai Terangan and also in the confluence of Sungai Tui and Sungai Sentul.

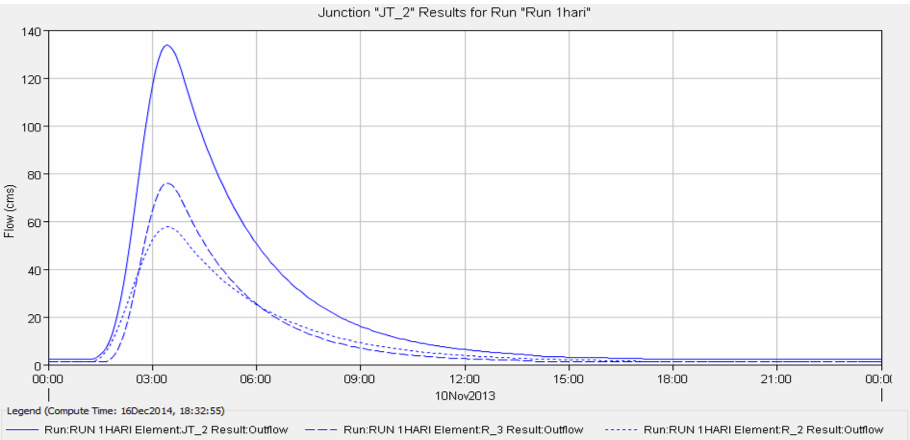

Figure 4.1: Flood discharge condition at JT2

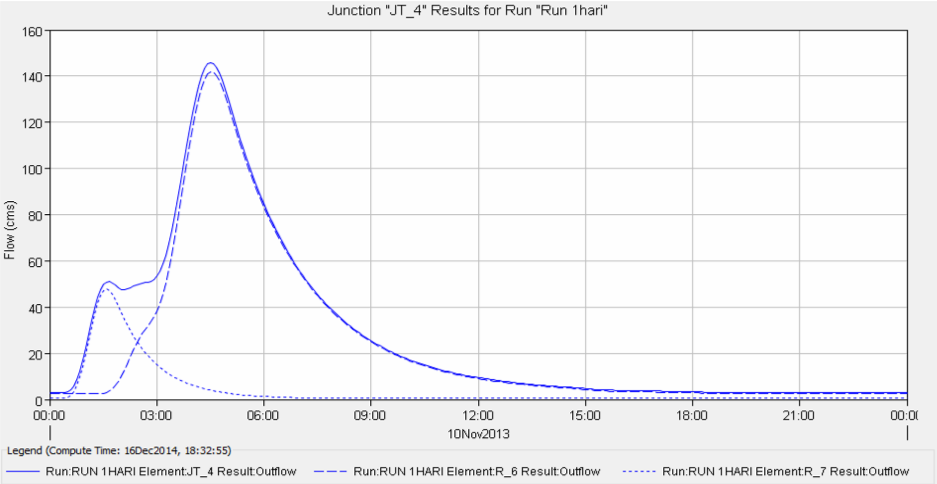

Figure 4.2: Flood discharge condition at JT4

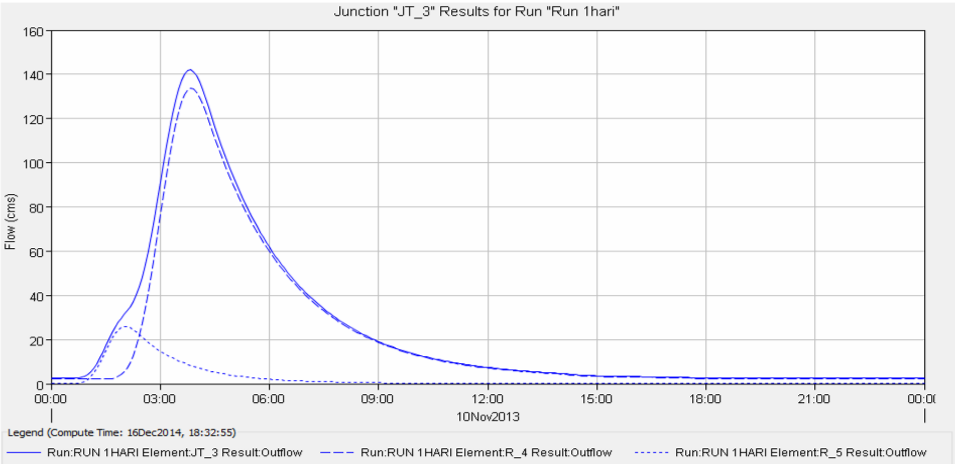

Figure 4.3: Flood discharge condition at JT3

Flood inundation due to rainfall event on November 9, 2013 will be generated by using calibrated HEC RAS model and the result of analysis shown in figures 4.4 below. Figure 4.5 shows water surface profile of Sungai Tui due to 127 mm accumulation depth on November 9, 2013 and water level generated of Ch. 2350.

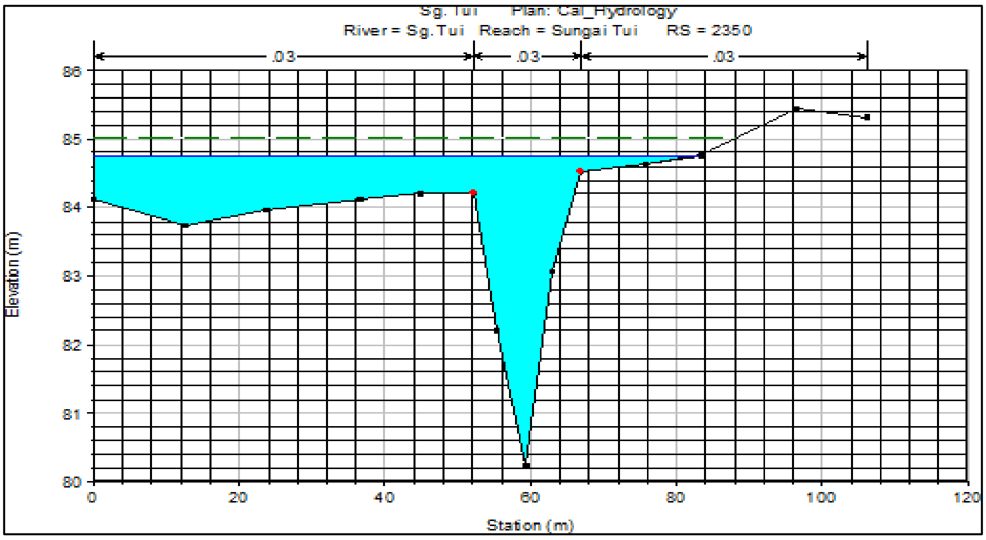

Figure 4.4: Cross section of channel 2350

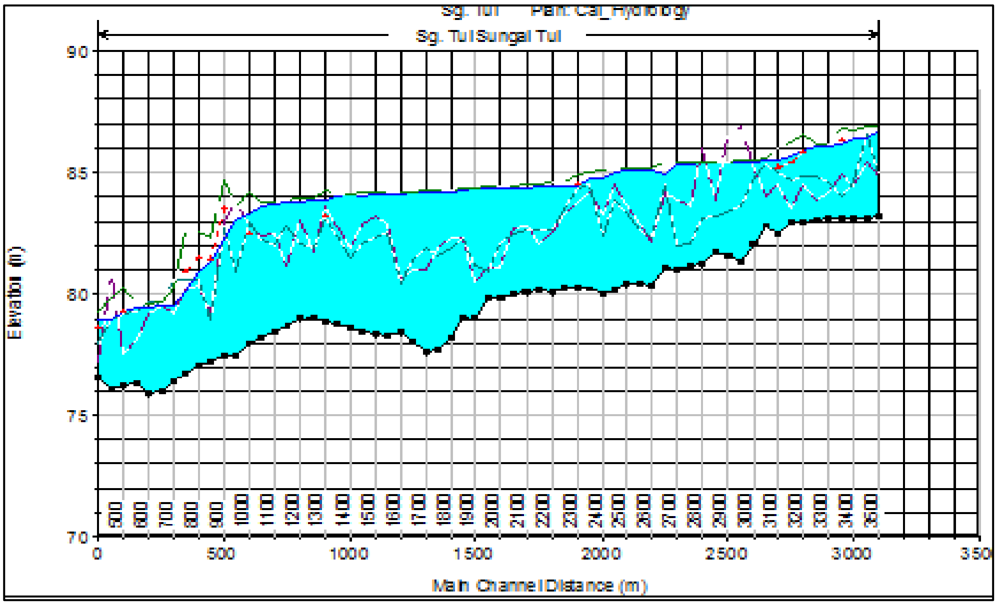

Figure 4.5: Water surface profile

Based on topographic survey the house level is at the elevation 84.117 and the inundation level was at 84.76, so the depth of inundation was at 0.643 m. When we see on Figure below, the inundation depth was around 0.6 m. It can be concluded that HEC HMS with Clark Methods can be used for Sungai Tui.

Figure 4.6: Inundation depth

4.1.2 YEARLY STREAM FLOW GENERATION

Stream flow can be generated using HEC HMS from JAN to DEC of the year 1999. Stream flow generated at junction 2 (JT2) of river station 3500 can be seen in the figures below.

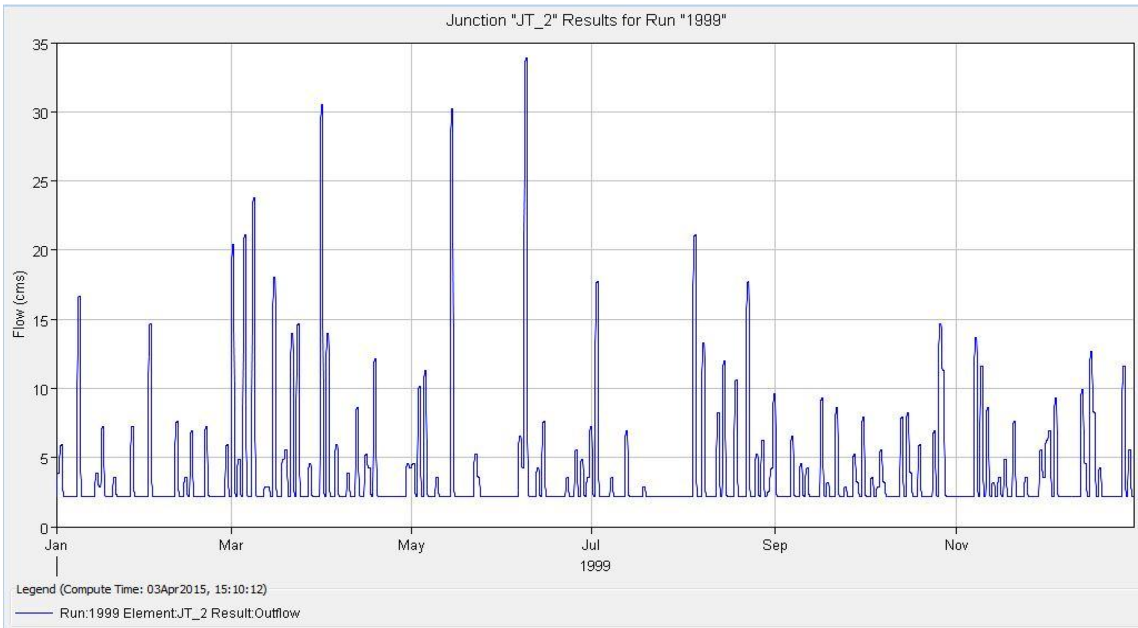

Figure 4.7: Stream flow at JT2 (RS 3500)

Lateral flow generated at reach 5 (R5) of river station 2450 and reach 7 (R7) of river station 850 can be seen in the figures below.

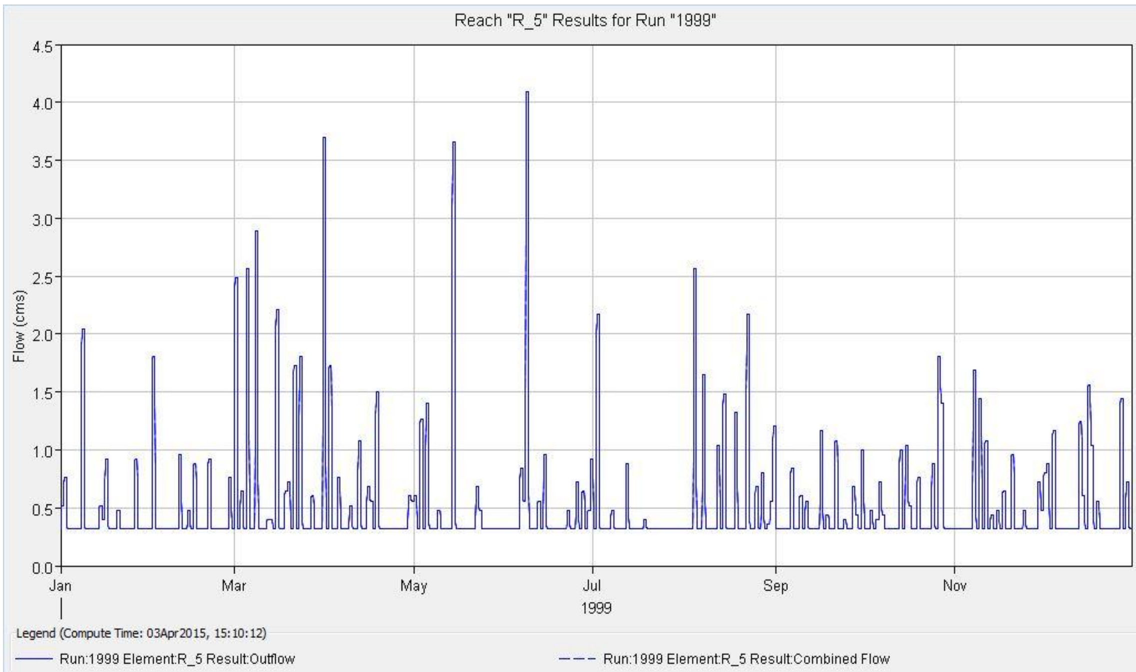

Figure 4.8: Lateral flow at R5 (RS 2450)

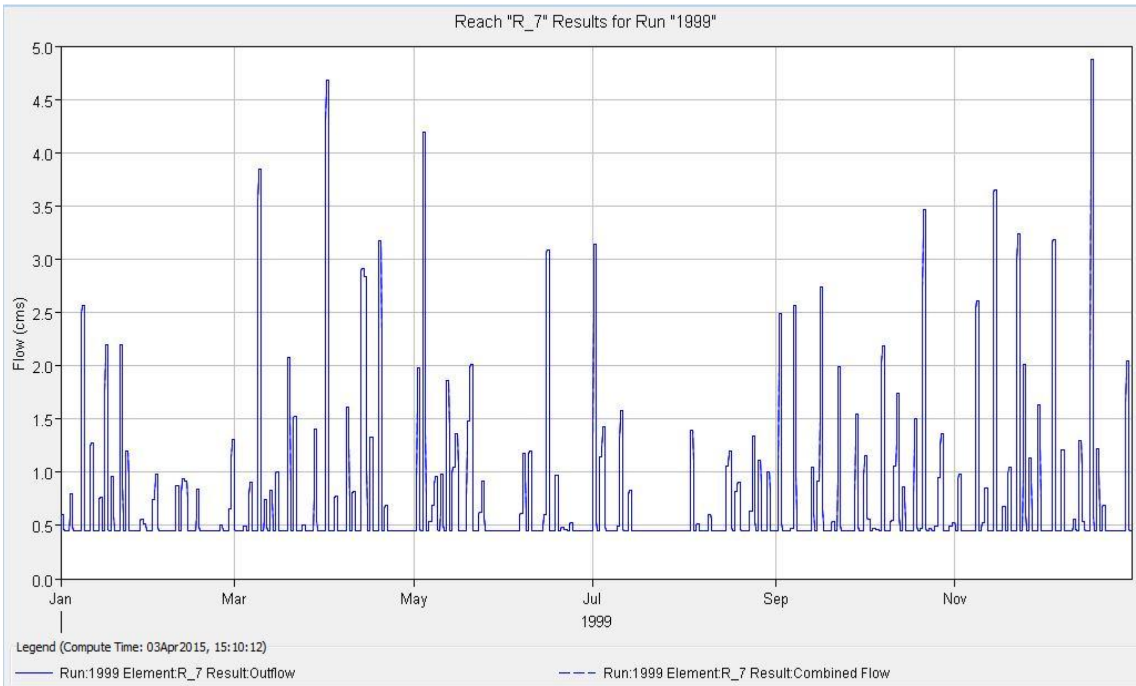

Figure 4.9: Lateral flow at R7 (RS 850)

4.2 SEDIMENT TRANSPORT ANALYSIS FOR 1 YEAR

4.2.1 Ackers-White

The elevation of the bed stream changes from 80.14 m to 80.12 m at the cross section of 2450 (75 m from upstream bridge). Erosion occurs at the depth of 0.02 m. The elevation of the bed stream changes from 80.03 m to 79.94m at the cross section of 2400 (25 m from upstream bridge). Erosion occurs at the depth of 0.09m. The elevation of the bed stream changes from 80.23 m to 79.81 m at the cross section of 2350 (25 m from downstream bridge). Erosion occurs at the depth of 0.42 m. The elevation of the bed stream changes from 80.28 m to 79.8 m at the cross section of 2300 (75 m from downstream bridge). Erosion occurs at the depth of 0.48 m.

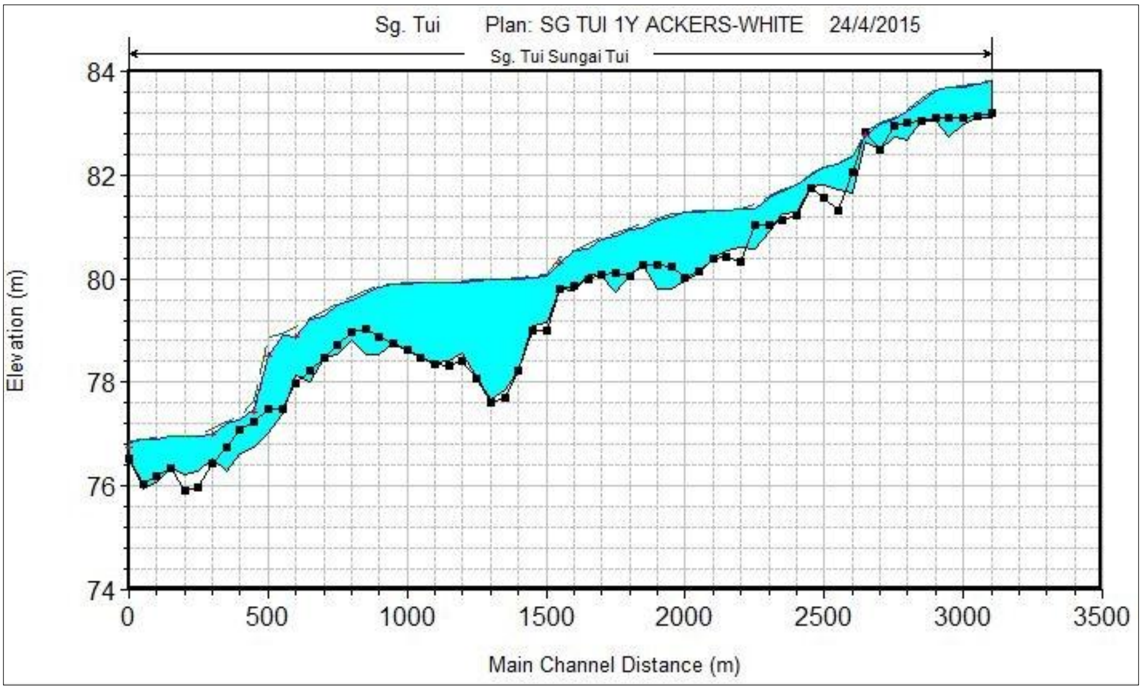

Figure 4.10: Water surface profile of sediment transport using the method of Ackers-White for 1 year analysis

4.2.2 England-Hansen

The elevation of the bed stream changes from 80.14 m to 80.17 m at the cross section of 2450 (75 m from upstream bridge). Deposition occurs at the depth of 0.03 m. The elevation of the bed stream changes from 80.03 m to 79.55 m at the cross section of 2400 (25 m from upstream bridge). Erosion occurs at the depth of 0.48 m. The elevation of the bed stream changes from 80.23 m to 79.75 m at the cross section of 2350 (25 m from downstream bridge). Erosion occurs at the depth of 0.48 m. The elevation of the bed stream changes from 80.28 m to 79.79 m at the cross section of 2300 (75 m from downstream bridge). Erosion occurs at the depth of 0.49 m.

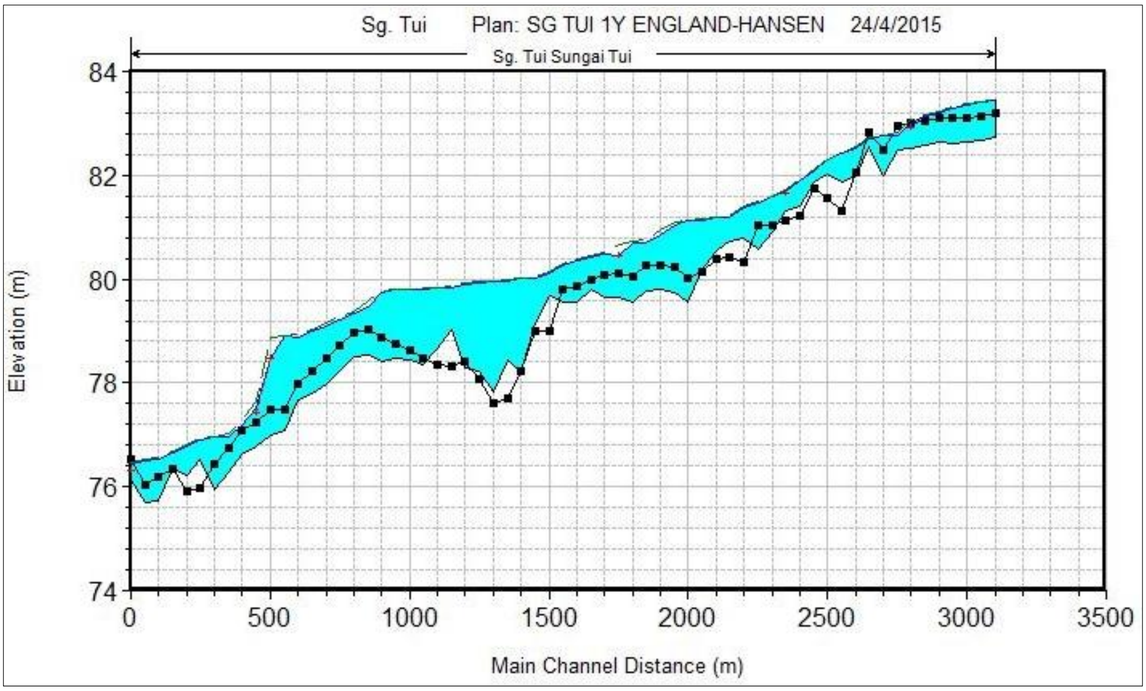

Figure 4.11: Water surface profile of sediment transport using the method of England-Hansen for 1 year analysis

4.2.3 Laursen

The elevation of the bed stream changes from 80.14 m to 80.34 m at the cross section of 2450 (75 m from upstream bridge). Deposition occurs at the depth of 0.20 m. The elevation of the bed stream changes from 80.03 m to 79.64 m at the cross section of 2400 (25 m from upstream bridge). Erosion occurs at the depth of 0.39 m. The elevation of the bed stream changes from 80.23 m to 79.74 m at the cross section of 2350 (25 m from downstream bridge). Erosion occurs at the depth of 0.49 m. The elevation of the bed stream changes from 80.28 m to 79.79 m at the cross section of 2300 (75 m from downstream bridge). Erosion occurs at the depth of 0.49 m.

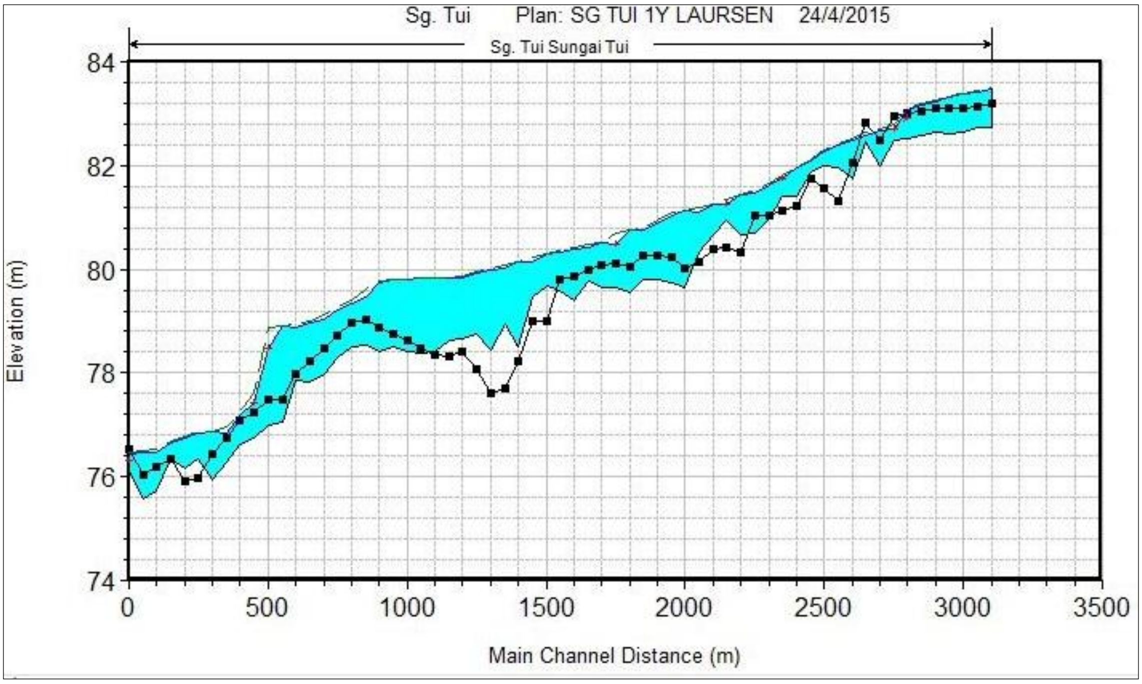

Figure 4.12: Water surface profile of sediment transport using the method of Laursen for 1 year analysis

4.2.4 Meyer Peter Muller

The elevation of the bed stream changes from 80.14 m to 80.11 m at the cross section of 2450 (75 m from upstream bridge). Erosion occurs at the depth of 0.03 m. The elevation of the bed stream changes from 80.03 m to 79.90 m at the cross section of 2400 (25 m from upstream bridge). Erosion occurs at the depth of 0.13 m. The elevation of the bed stream changes from 80.23 m to 79.74 m at the cross section of 2350 (25 m from downstream bridge). Erosion occurs at the depth of 0.49 m. The elevation of the bed stream changes from 80.28 m to 79.80 m at the cross section of 2300 (75 m from downstream bridge). Erosion occurs at the depth of 0.48 m.

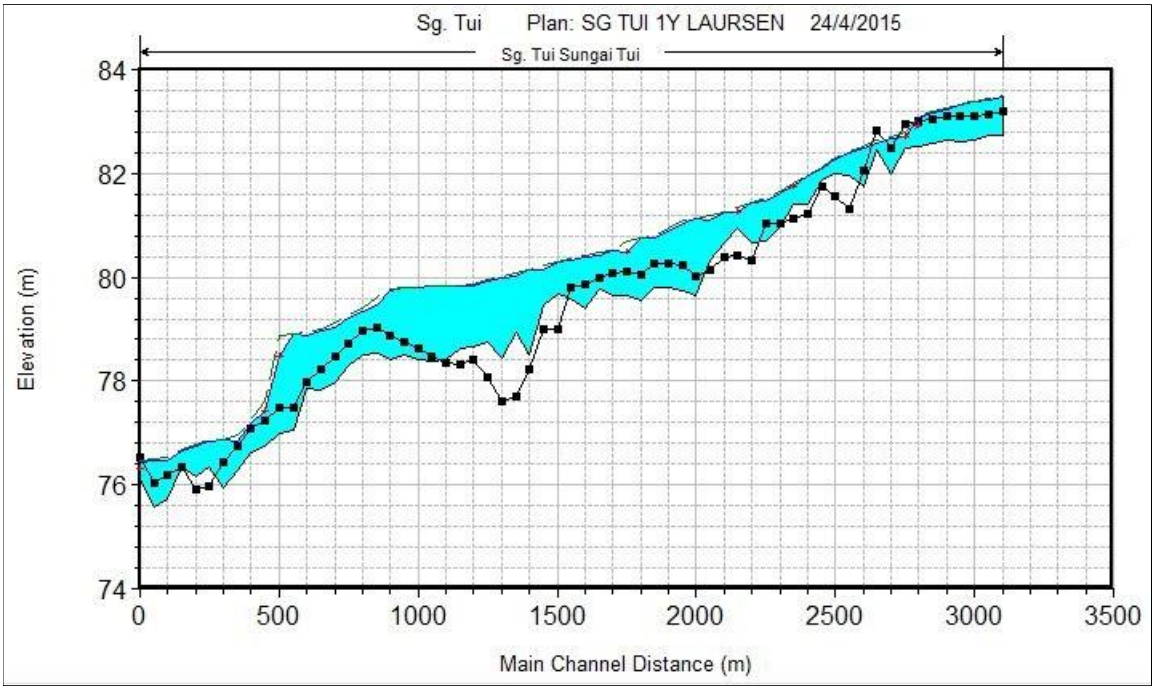

Figure 4.13: Water surface profile of sediment transport using the method of Meyer Peter Muller for 1 year analysis

4.2.5 Toffaleti

The elevation of the bed stream changes from 80.14 m to 80.12 m at the cross section of 2450 (75m from upstream bridge). Erosion occurs at the depth of 0.02 m. The elevation of the bed stream changes from 80.03 m to 80.01 m at the cross section of 2400 (25 m from upstream bridge). Erosion occurs at the depth of 0.02 m. The elevation of the bed stream changes from 80.23 m to 79.98 m at the cross section of 2350 (25 m from downstream bridge). Erosion occurs at the depth of 0.25 m. The elevation of the bed stream changes from 80.28 m to 80.02 m at the cross section of 2300 (75 m from downstream bridge). Erosion occurs at the depth of 0.26 m.

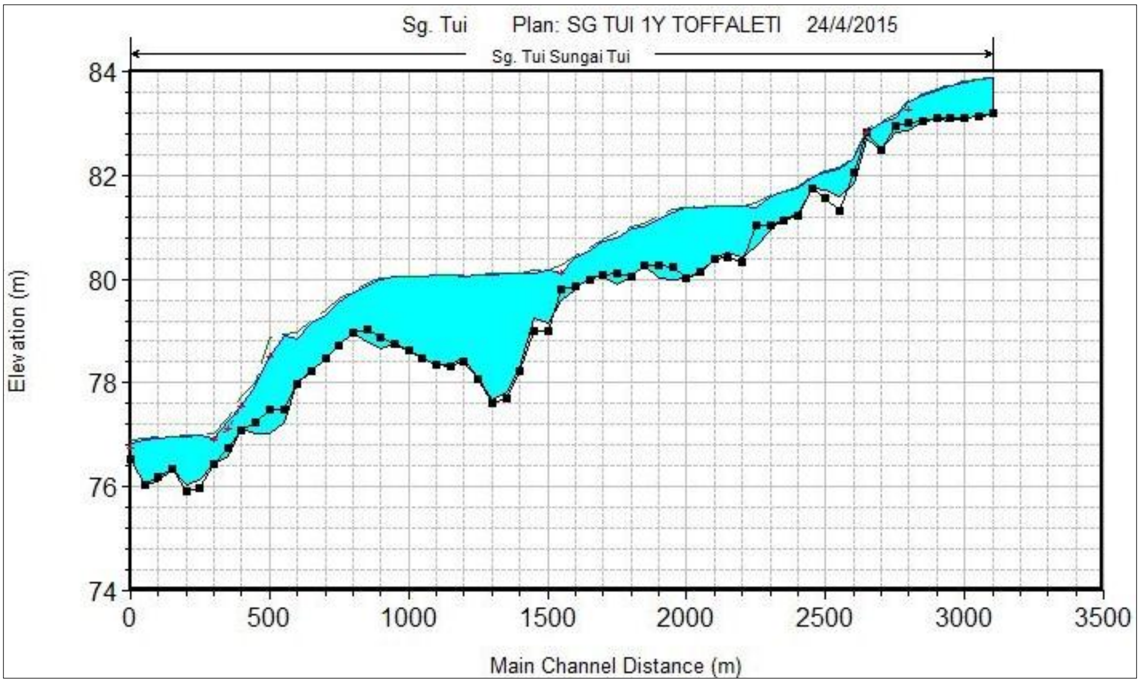

Figure 4.14: Water surface profile of sediment transport using the method of Toffaleti for 1 year analysis.

4.2.6 Wilcock

The elevation of the bed stream changes from 80.14 m to 80.13 m at the cross section of 2450 (75 m from upstream bridge). Erosion occurs at the depth of 0.01 m. The elevation of the bed stream changes from 80.03 m to 80.02 m at the cross section of 2400 (25 m from upstream bridge). Erosion occurs at the depth of 0.01 m. The elevation of the bed stream changes from 80.23 m to 80.17 m at the cross section of 2350 (25 m from downstream bridge). Erosion occurs at the depth of 0.06 m. The elevation of the bed stream changes from 80.28 m to 80.26 m at the cross section of 2300 (75 m from downstream bridge). Erosion occurs at the depth of 0.02 m.

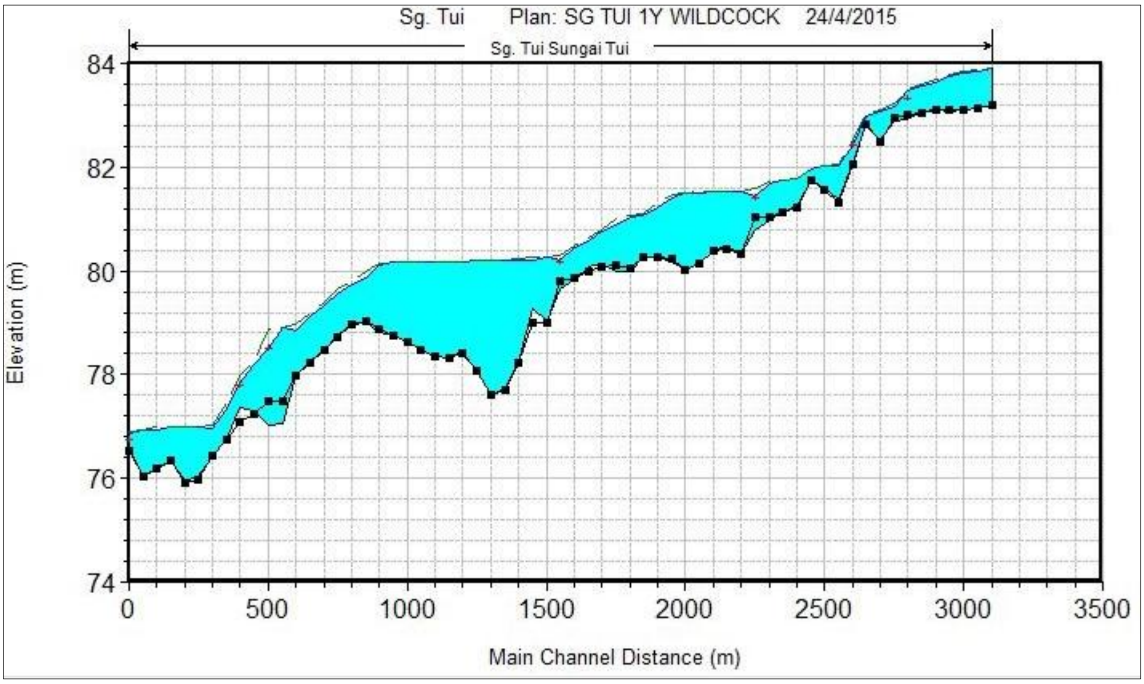

Figure 4.15: Water surface profile of sediment transport using the method of Wilcock for 1 year analysis.

4.2.7 Yang

The elevation of the bed stream changes from 80.14 m to 80.11 m at the cross section of 2450 (75 m from upstream bridge). Erosion occurs at the depth of 0.03 m. The elevation of the bed stream changes from 80.03 m to 79.94 m at the cross section of 2400 (25 m from upstream bridge). Erosion occurs at the depth of 0.09 m. The elevation of the bed stream changes from 80.23 m to 79.83 m at the cross section of 2350 (25 m from downstream bridge). Erosion occurs at the depth of 0.40 m. The elevation of the bed stream changes from 80.28 m to 80.28 m at the cross section of 2300 (75 m from downstream bridge). Deposition occurs at the depth of 0.03 m.

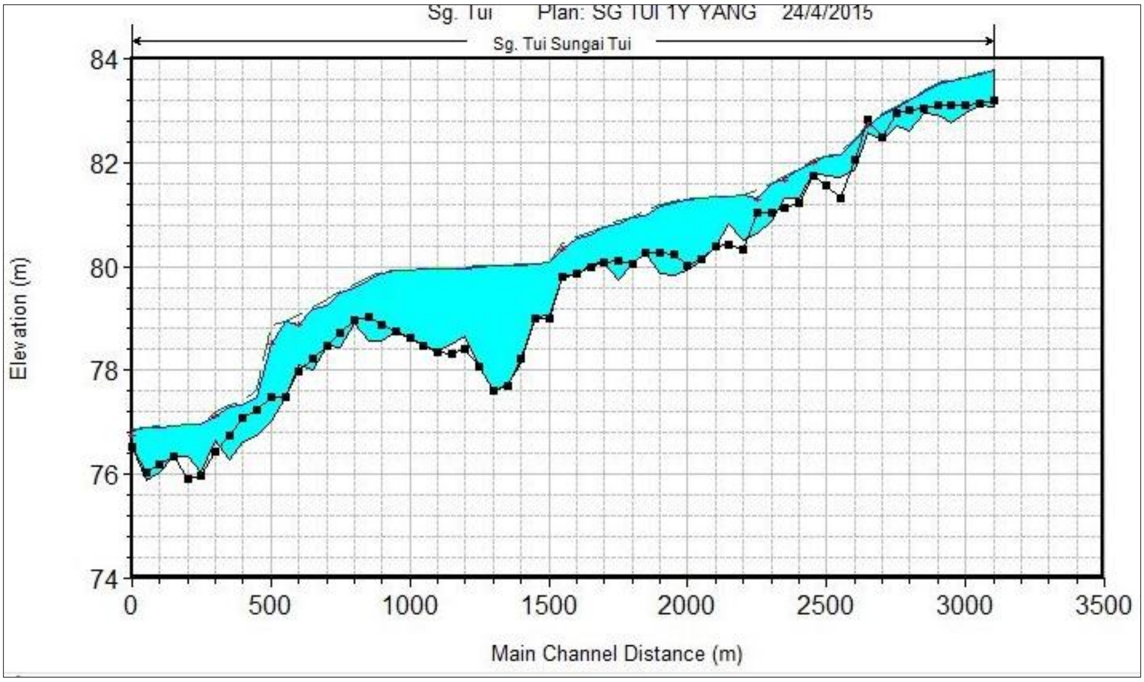

Figure 4.16: Water surface profile of sediment transport using the method of Yang for 1 year analysis.

4.3 SEDIMENT TRANSPORT ANALYSIS FOR 3 YEARS

4.3.1 Ackers-White

The elevation of the bed stream changes from 80.14 m to 80.15 m at the cross section of 2450 (75 m from upstream bridge). Deposition occurs at the depth of 0.01 m. The elevation of the bed stream changes from 80.03 m to 79.81 m at the cross section of 2400 (25 m from upstream bridge). Erosion occurs at the depth of 0.22 m. The elevation of the bed stream changes from 80.23 m to 79.75 m at the cross section of 2350 (25 m from downstream bridge). Erosion occurs at the depth of 0.48 m. The elevation of the bed stream changes from 80.28 m to 79.8 m at the cross section of 2300 (75 m from downstream bridge). Erosion occurs at the depth of 0.48 m.

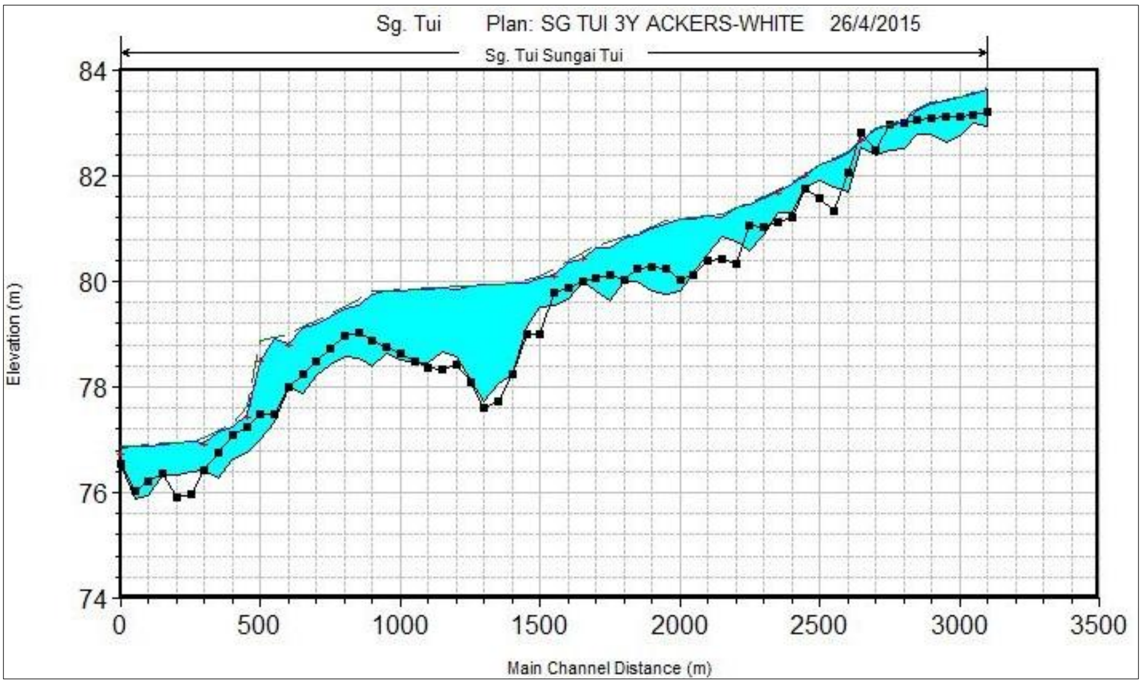

Figure 4.17: Pattern of sediment transport using the method of Ackers-White for 3 years analysis.

4.3.2 England-Hansen

The elevation of the bed stream changes from 80.14 m to 80.13 m at the cross section of 2450 (75 m from upstream bridge). Erosion occurs at the depth of 0.01 m. The elevation of the bed stream changes from 80.03 m to 79.55 m at the cross section of 2400 (25 m from upstream bridge). Erosion occurs at the depth of 0.48m. The elevation of the bed stream changes from 80.23 m to 79.74 m at the cross section of 2350 (25 m from downstream bridge). Erosion occurs at the depth of 0.49 m. The elevation of the bed stream changes from 80.28 m to 79.79 m at the cross section of 2300 (75 m from downstream bridge). Erosion occurs at the depth of 0.49 m.

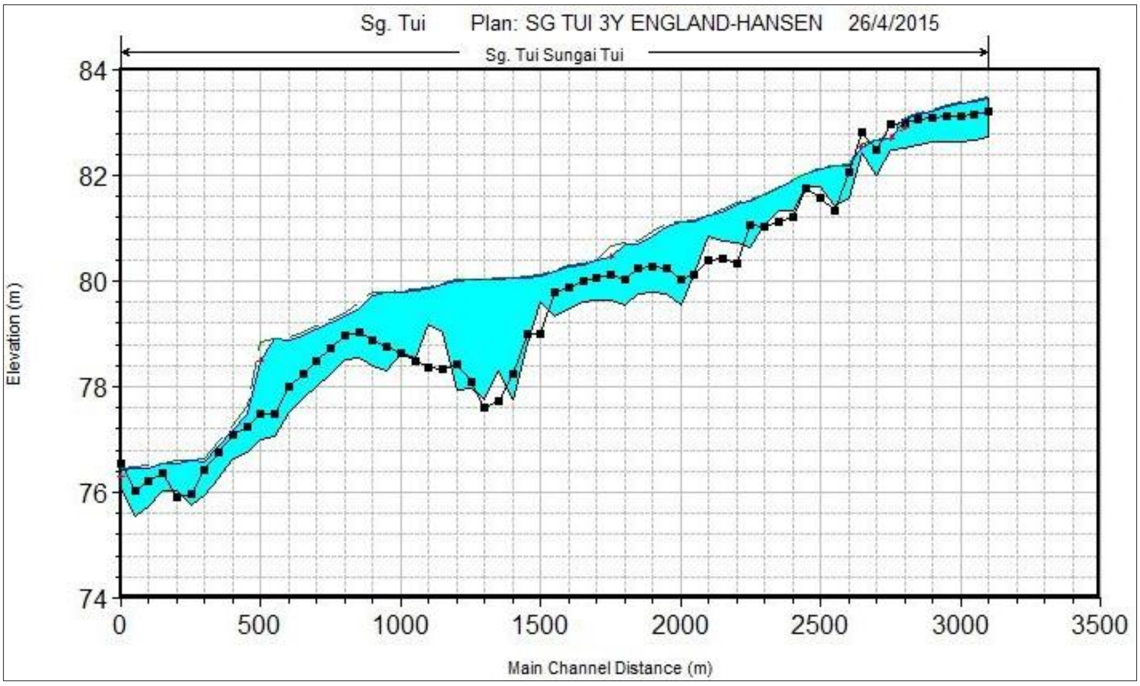

Figure 4.18: Pattern of sediment transport using the method of England-Hansen for 3 years analysis.

4.3.3 Laursen

The elevation of the bed stream changes from 80.14 m to 80.31 m at the cross section of 2450 (75 m from upstream bridge). Deposition occurs at the depth of 0.17 m. The elevation of the bed stream changes from 80.03 m to 79.88 m at the cross section of 2400 (25 m from upstream bridge). Erosion occurs at the depth of 0.15 m. The elevation of the bed stream changes from 80.23 m to 79.74 m at the cross section of 2350 (25 m from downstream bridge). Erosion occurs at the depth of 0.49 m. The elevation of the bed stream changes from 80.28m to 79.79 m at the cross section of 2300 (75 m from downstream bridge). Erosion occurs at the depth of 0.49 m.

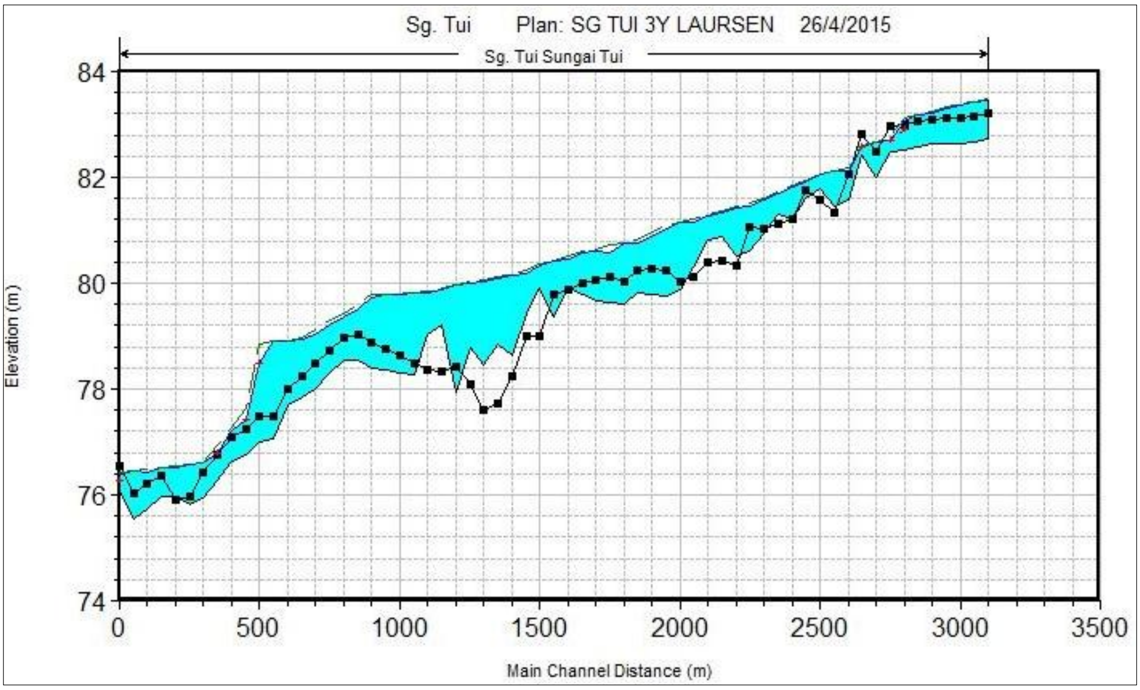

Figure 4.10: Pattern of sediment transport using the method of Laursen for 3 years analysis

4.3.4 Meyer Peter Muller

The elevation of the bed stream changes from 80.14 m to 80.33 m at the cross section of 2450 (75 m from upstream bridge). Deposition occurs at the depth of 0.19 m. The elevation of the bed stream changes from 80.03 m to 79.77 m at the cross section of 2400 (25 m from upstream bridge). Erosion occurs at the depth of 0.26 m. The elevation of the bed stream changes from 80.23 m to 79.75 m at the cross section of 2350 (25 m from downstream bridge). Erosion occurs at the depth of 0.48 m. The elevation of the bed stream changes from 80.28 m to 79.81 m at the cross section of 2300 (75 m from downstream bridge). Erosion occurs at the depth of 0.47 m.

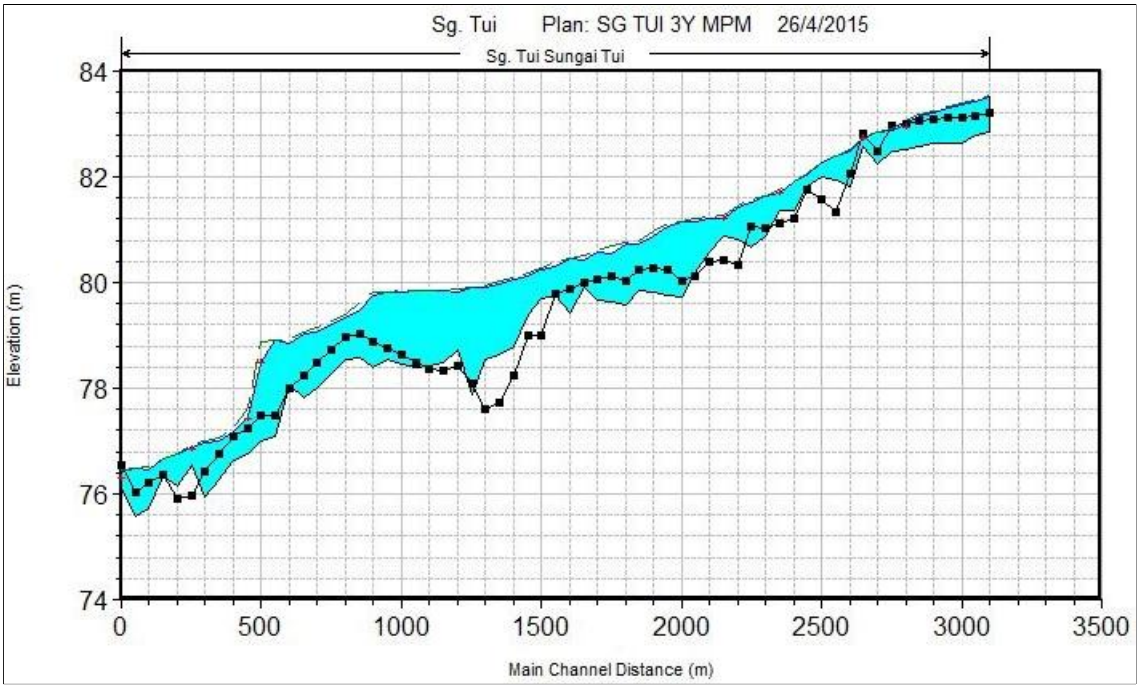

Figure 4.11: Water surface profile of sediment transport using the method of Meyer Peter Muller for 3 years analysis

4.3.5 Toffaleti

The elevation of the bed stream changes from 80.14 m to 80.10 m at the cross section of 2450 (75 m from upstream bridge). Erosion occurs at the depth of 0.04 m. The elevation of the bed stream changes from 80.03 m to 79.95 m at the cross section of 2400 (25 m from upstream bridge). Erosion occurs at the depth of 0.08 m. The elevation of the bed stream changes from 80.23 m to 79.84 m at the cross section of 2350 (25 m from downstream bridge). Erosion occurs at the depth of 0.39 m. The elevation of the bed stream changes from 80.28 m to 79.90 m at the cross section of 2300 (75 m from downstream bridge). Erosion occurs at the depth of 0.38 m.

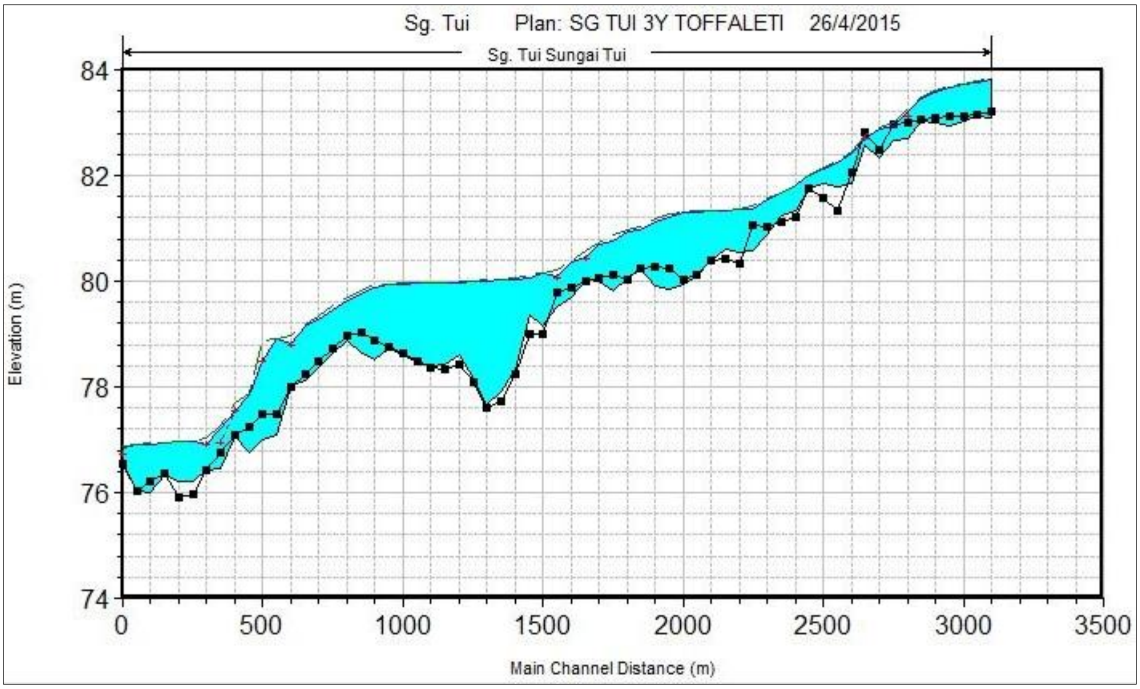

Figure 4.12: Pattern of sediment transport using the method of Toffaleti for 3 years analysis

4.3.6 Wilcock

The elevation of the bed stream changes from 80.14 m to 80.13 m at the cross section of 2450 (75 m from upstream bridge). Erosion occurs at the depth of 0.01 m. The elevation of the bed stream changes from 80.03 m to 79.99 m at the cross section of 2400 (25 m from upstream bridge). Erosion occurs at the depth of 0.04 m. The elevation of the bed stream changes from 80.23 m to 80.08 m at the cross section of 2350 (25 m from downstream bridge). Erosion occurs at the depth of 0.15 m. The elevation of the bed stream changes from 80.28 m to 80.25 m at the cross section of 2300 (75 m from downstream bridge). Erosion occurs at the depth of 0.03 m.

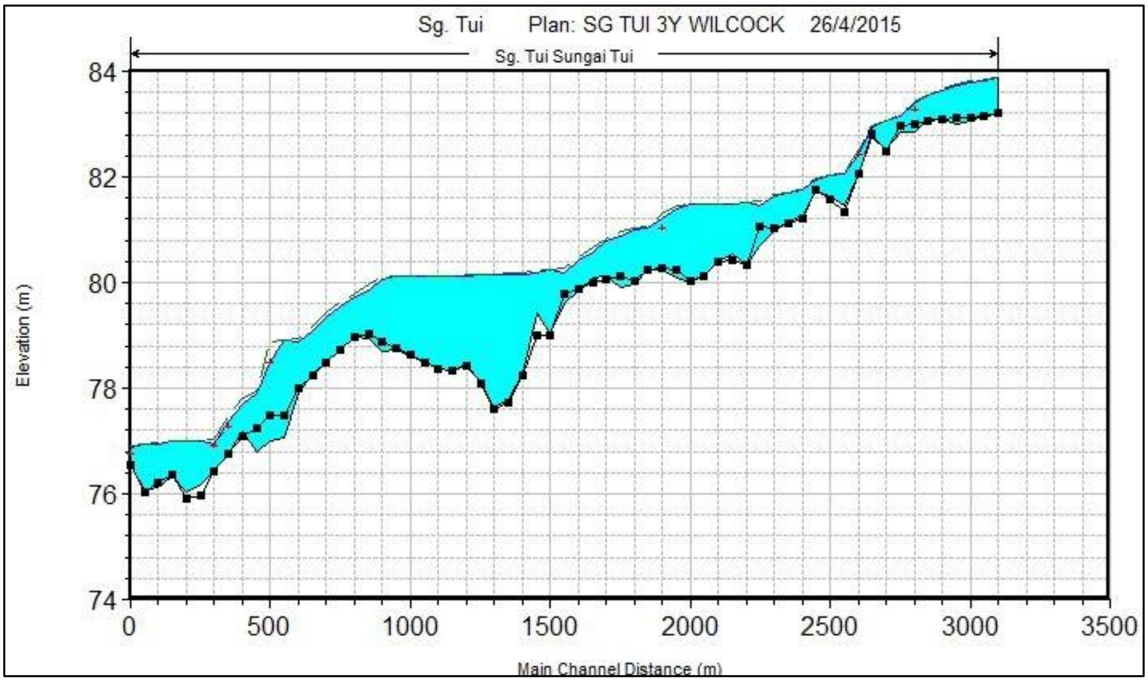

Figure 4.13: Pattern of sediment transport using the method of Wilcock for 3 years analysis

4.3.7 Yang

The elevation of the bed stream changes from 80.14 m to 80.33 m at the cross section of 2450 (75 m from upstream bridge). Deposition occurs at the depth of 0.19 m. The elevation of the bed stream changes from 80.03 m to 79.77 m at the cross section of 2400 (25 m from upstream bridge). Erosion occurs at the depth of 0.26 m. The elevation of the bed stream changes from 80.23 m to 79.75 m at the cross section of 2350 (25 m from downstream bridge). Erosion occurs at the depth of 0.48 m. The elevation of the bed stream changes from 80.28 m to 79.81 m at the cross section of 2300 (75 m from downstream bridge). Erosion occurs at the depth of 0.47 m.

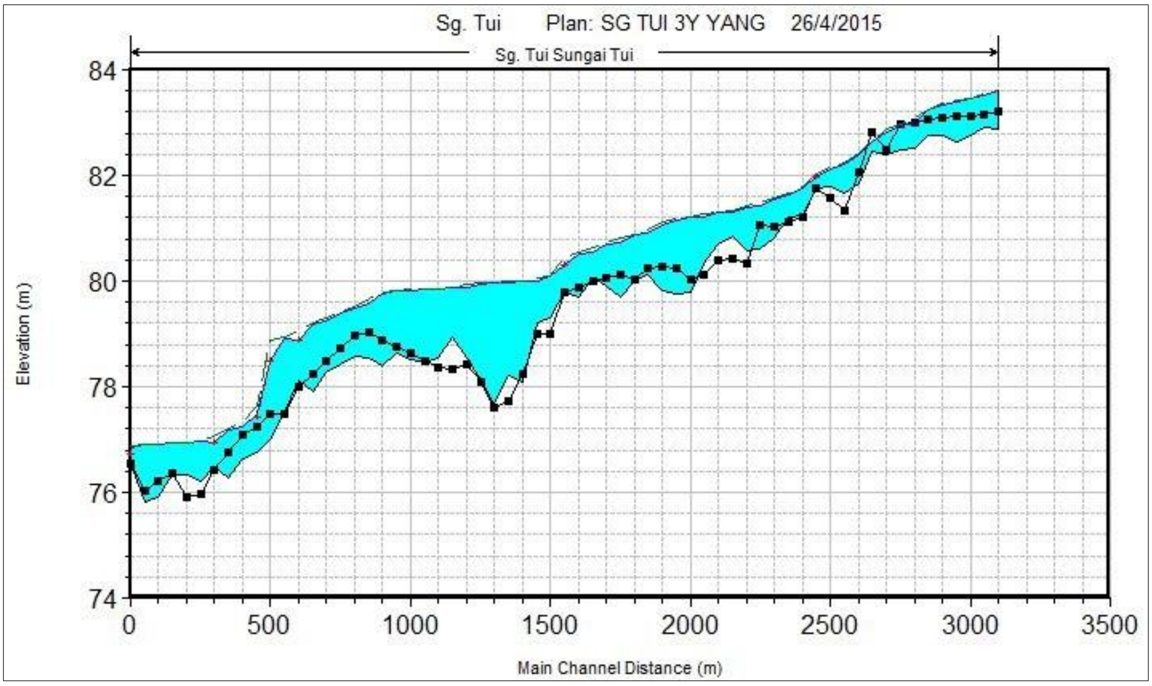

Figure 4.14: Pattern of sediment transport using the method of Yang for 3 years analysis

4.4 SEDIMENT TRANSPORT ANALYSIS FOR 5 YEARS

4.4.1 Ackers-White

The elevation of the bed stream changes from 80.14 m to 80.22 m at the cross section of 2450 (75 m from upstream bridge). Erosion occurs at the depth of 0.08 m. The elevation of the bed stream changes from 80.03 m to 79.72 m at the cross section of 2400 (25 m from upstream bridge). Deposition occurs at the depth of 0.31 m. The elevation of the bed stream changes from 80.23 m to 79.74 m at the cross section of 2350 (25 m from downstream bridge). Erosion occurs at the depth of 0.49 m. The elevation of the bed stream changes from 80.28 m to 79.82 m at the cross section of 2300 (75 m from downstream bridge). Erosion occurs at the depth of 0.46 m.

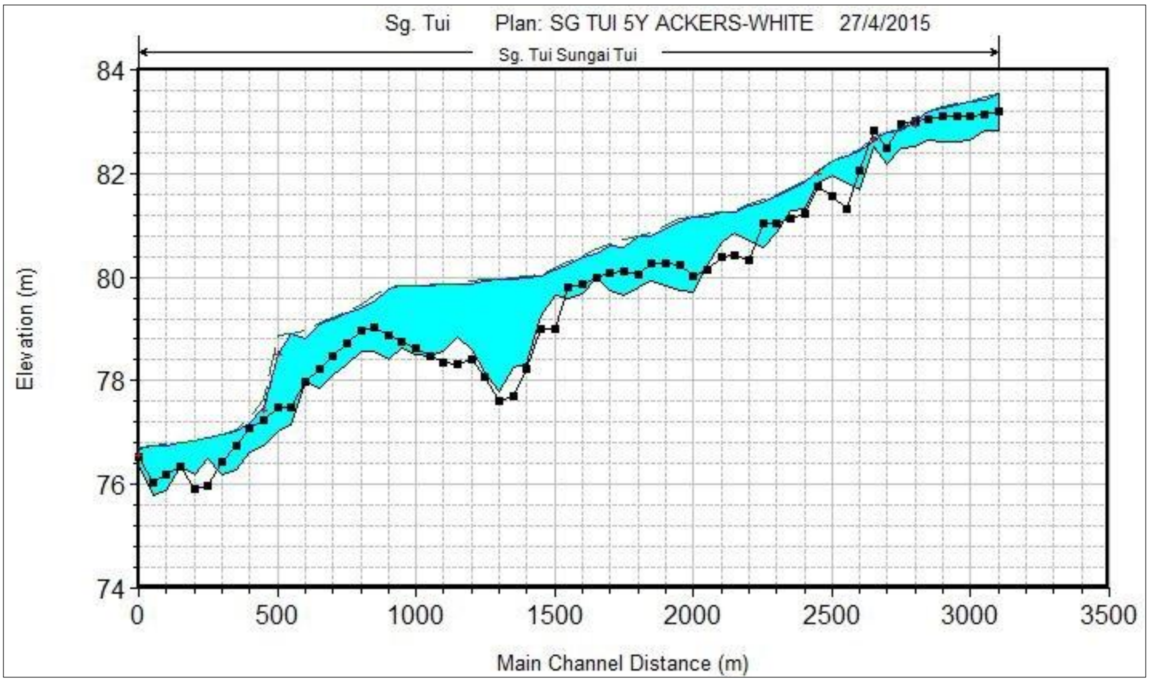

Figure 4.15: Pattern of sediment transport using the method of Ackers-White for 5 years analysis

4.4.2 England-Hansen

At the cross section of 2450 (75 m from upstream bridge), the elevation of the bed stream changes from 80.14 m to 80.11 m. Erosion occurs at the depth of 0.03 m. At the cross section of 2400 (25 m from upstream bridge), the elevation of the bed stream changes from 80.03 m to 79.55 m. Erosion occurs at the depth of 0.48 m. At the cross section of 2350 (25 m from downstream bridge), the elevation of the bed stream changes from 80.23 m to 79.74 m. Erosion occurs at the depth of 0.49 m. At the cross section of 2300 (75 m from downstream bridge), the elevation of the bed stream changes from 80.28 m to 79.79 m. Erosion occurs at the depth of 0.49 m.

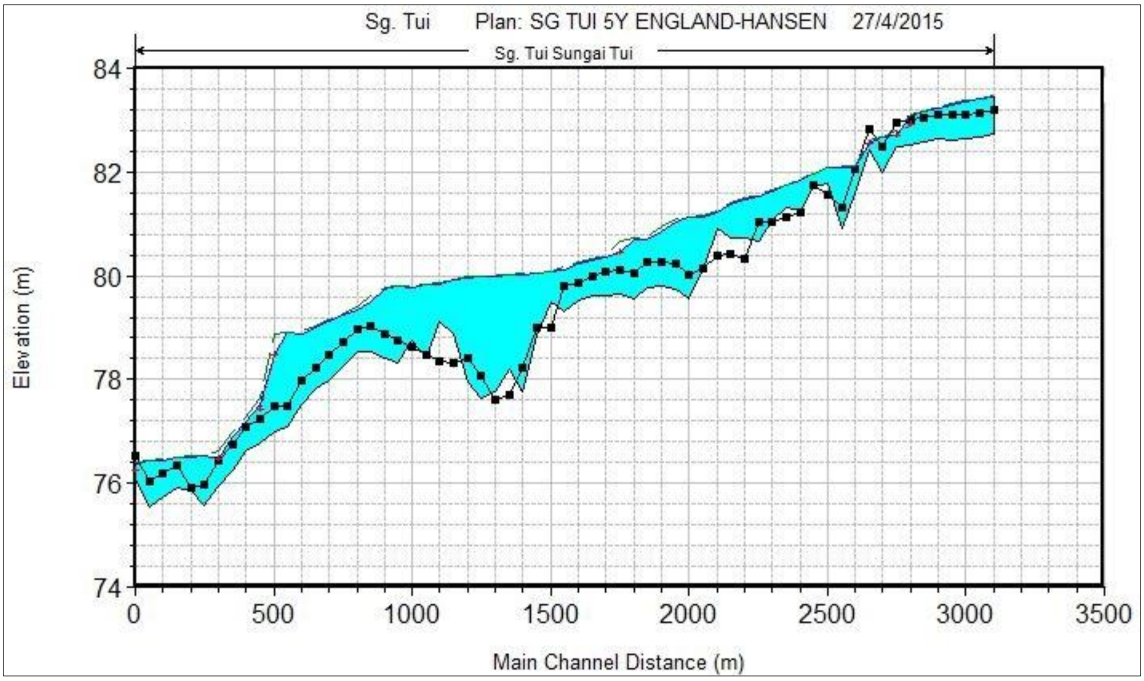

Figure 4.16: Pattern of sediment transport using the method of England-Hansen for 5 years analysis

4.4.3 Laursen

At the cross section of 2450 (75 m from upstream bridge), the elevation of the bed stream changes from 80.14 m to 80.30 m. Deposition occurs at the depth of 0.16 m. At the cross section of 2400 (25 m from upstream bridge), the elevation of the bed stream changes from 80.03 m to 79.80 m. Erosion occurs at the depth of 0.23 m. At the cross section of 2350 (25 m from downstream bridge), the elevation of the bed stream changes from 80.23 m to 79.74 m. Erosion occurs at the depth of 0.49 m. At the cross section of 2300 (75 m from downstream bridge), the elevation of the bed stream changes from 80.28 m to 79.85 m. Erosion occurs at the depth of 0.43 m.

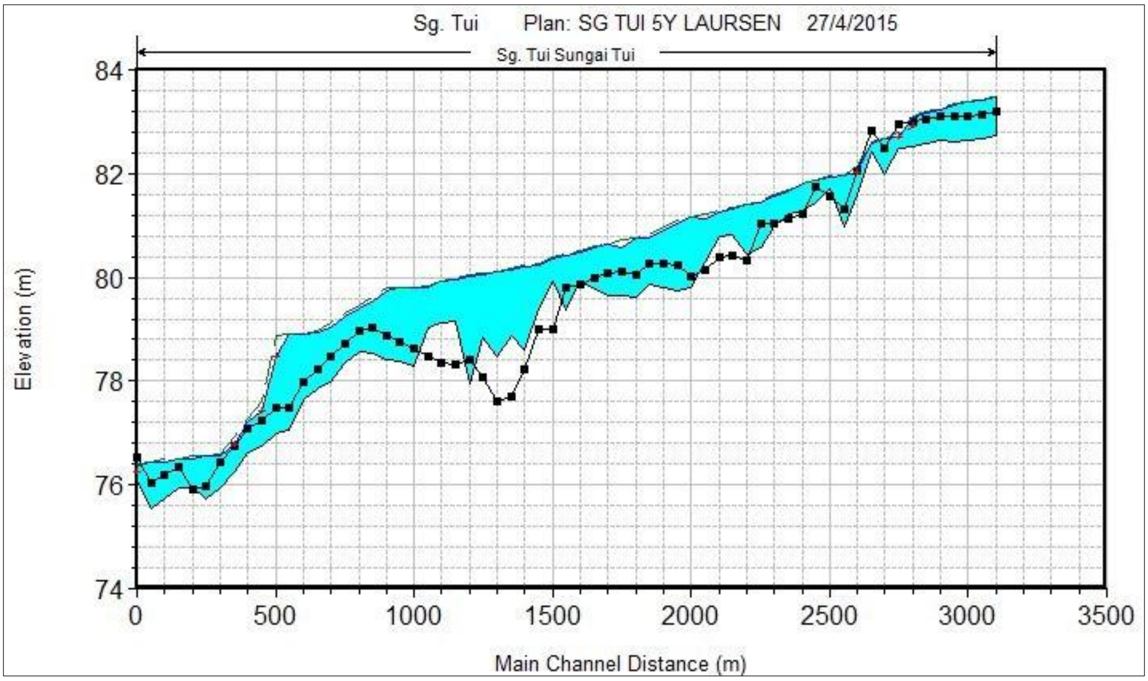

Figure 4.17: Pattern of sediment transport using the method of Laursen for 5 years analysis.

4.4.4 Meyer Peter Muller

At the cross section of 2450 (75 m from upstream bridge), the elevation of the bed stream changes from 80.14 m to 80.30 m. Deposition occurs at the depth of 0.16 m. At the cross section of 2400 (25 m from upstream bridge), the elevation of the bed stream changes from 80.03 m to 79.80 m. Erosion occurs at the depth of 0.23 m. At the cross section of 2350 (25 m from downstream bridge), the elevation of the bed stream changes from 80.23 m to 79.74 m. Erosion occurs at the depth of 0.49 m. At the cross section of 2300 (75 m from downstream bridge), the elevation of the bed stream changes from 80.28 m to 79.85 m. Erosion occurs at the depth of 0.43 m.

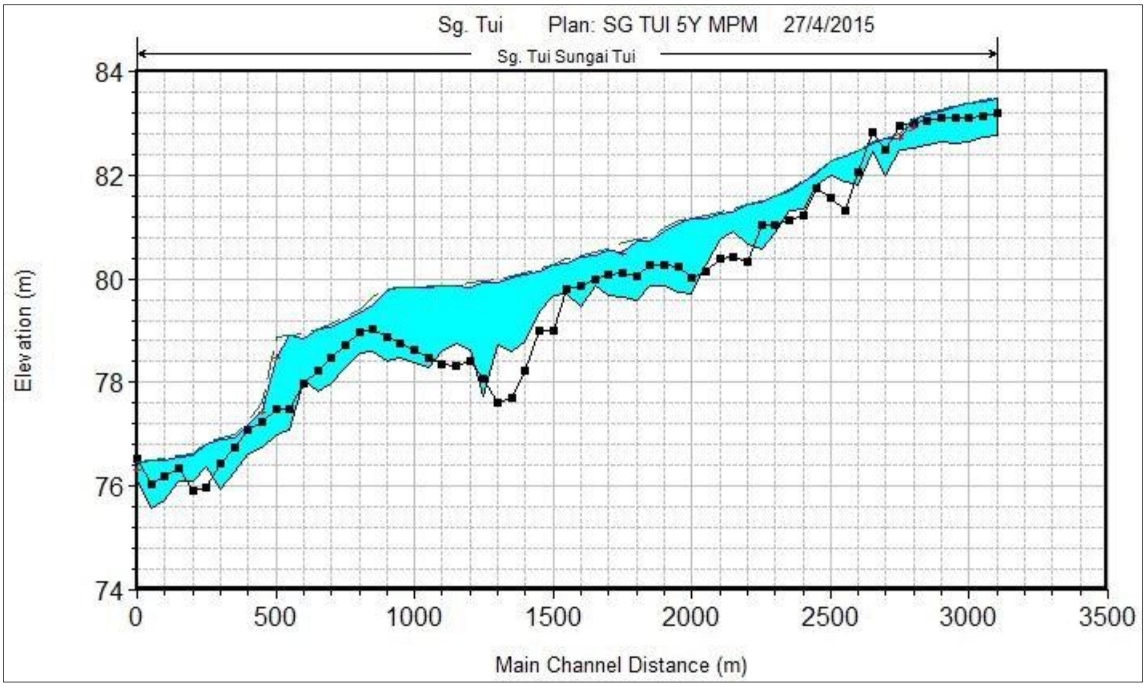

Figure 4.18: Pattern of sediment transport using the method of Meyer Peter Muller for 5 years analysis

4.4.5 Toffaleti

At the cross section of 2450 (75 m from upstream bridge), the elevation of the bed stream changes from 80.14 m to 80.06 m. Erosion occurs at the depth of 0.08 m. At the cross section of 2400 (25 m from upstream bridge), the elevation of the bed stream changes from 80.03 m to 79.90 m. Erosion occurs at the depth of 0.13 m. At the cross section of 2350 (25 m from downstream bridge), the elevation of the bed stream changes from 80.23 m to 79.78 m. Erosion occurs at the depth of 0.45 m. At the cross section of 2300 (75 m from downstream bridge), the elevation of the bed stream changes from 80.28 m to 79.82 m. Erosion occurs at the depth of 0.46 m.

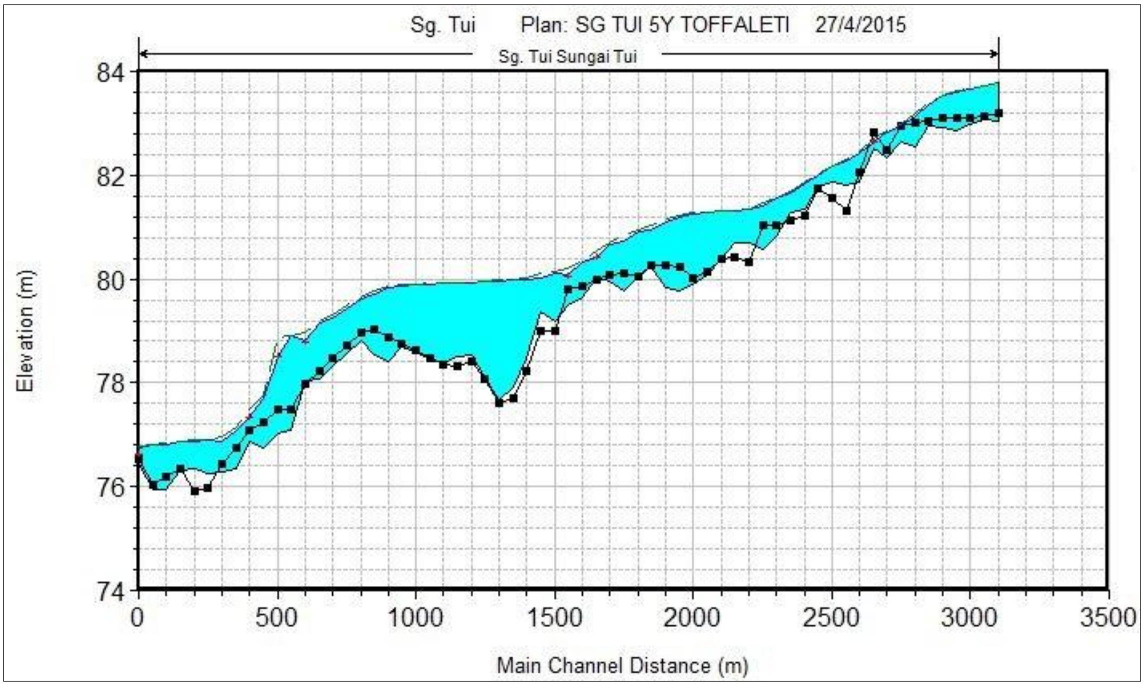

Figure 4.19: Pattern of sediment transport using the method of Toffaleti for 5 years analysis

4.4.6 Wilcock

At the cross section of 2450 (75 m from upstream bridge), the elevation of the bed stream changes from 80.14 m to 80.13 m. Erosion occurs at the depth of 0.01 m. At the cross section of 2400 (25 m from upstream bridge), the elevation of the bed stream changes from 80.03 m to 79.97 m. Erosion occurs at the depth of 0.06 m. At the cross section of 2350 (25 m from downstream bridge), the elevation of the bed stream changes from 80.23 m to 80.00 m. Erosion occurs at the depth of 0.23 m. At the cross section of 2300 (75 m from downstream bridge), the elevation of the bed stream changes from 80.28 m to 80.25 m. Erosion occurs at the depth of 0.03 m.

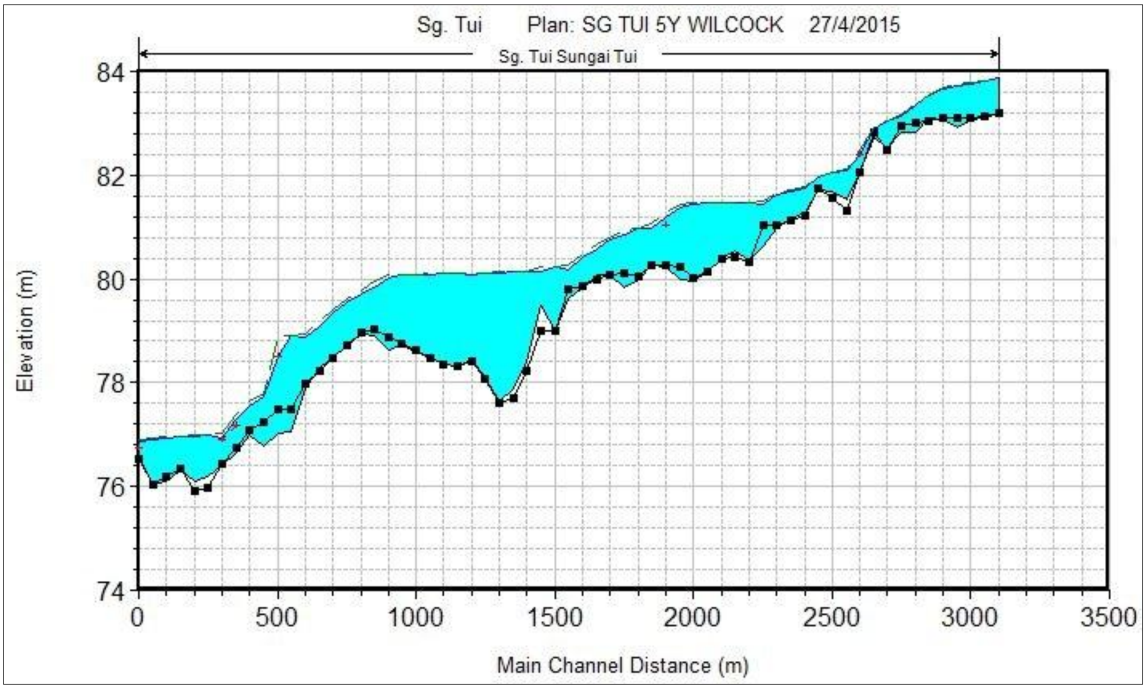

Figure 4.20: Pattern of sediment transport using the method of Wilcock for 5 years analysis

4.4.7 Yang

At the cross section of 2450 (75 m from upstream bridge), the elevation of the bed stream changes from 80.14 m to 80.19 m. Deposition occurs at the depth of 0.05 m. At the cross section of 2400 (25 m from upstream bridge), the elevation of the bed stream changes from 80.03 m to 79.68 m. Erosion occurs at the depth of 0.35 m. At the cross section of 2350 (25 m from downstream bridge), the elevation of the bed stream changes from 80.23 m to 79.75 m. Erosion occurs at the depth of 0.48 m. At the cross section of 2300 (75 m from downstream bridge), the elevation of the bed stream changes from 80.28 m to 79.81 m. Erosion occurs at the depth of 0.47 m.

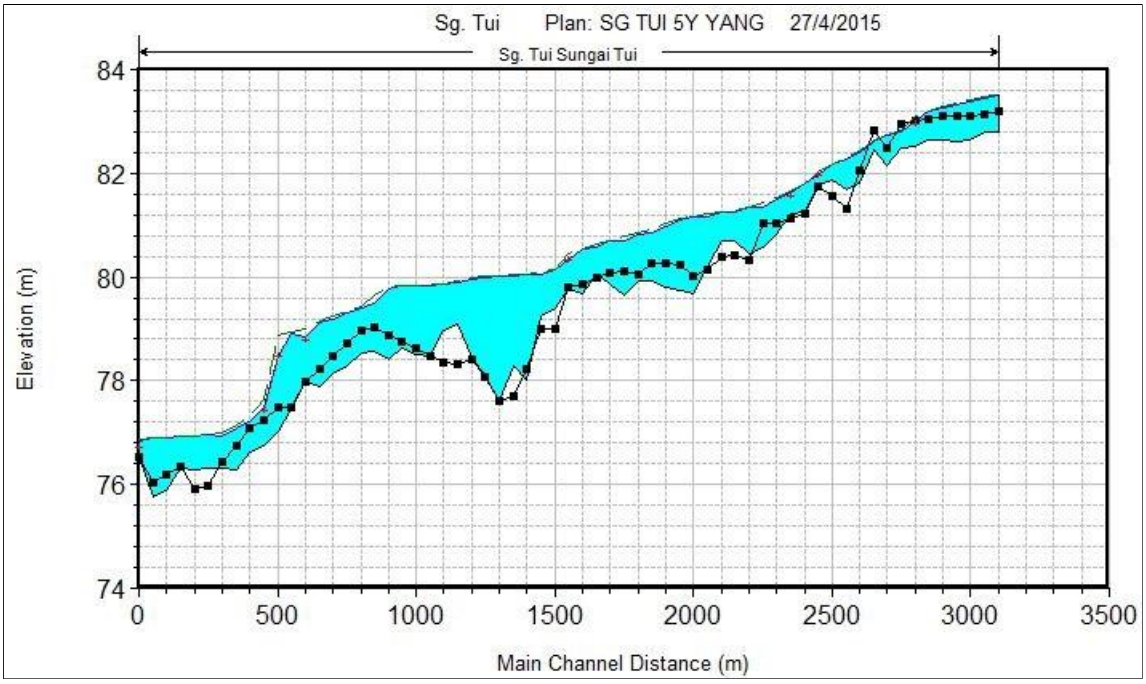

Figure 4.21: Pattern of sediment transport using the method of Yang for 5 years analysis

4.5 SEDIMENT TRANSPORT ANALYSIS FOR 10 YEARS

4.5.1 Ackers-White

The elevation of the bed stream changes from 80.14 m to 80.24 m at the cross section of 2450 (75 m from upstream bridge). Deposition occurs at the depth of 0.10 m. The elevation of the bed stream changes from 80.03 m to 79.60 m at the cross section of 2400 (25 m from upstream bridge). Erosion occurs at the depth of 0.43 m. The elevation of the bed stream changes from 80.23 m to 79.75 m at the cross section of 2350 (25 m from downstream bridge). Erosion occurs at the depth of 0.48 m. The elevation of the bed stream changes from 80.28 m to 79.79 m at the cross section of 2300 (75 m from downstream bridge). Erosion occurs at the depth of 0.49 m.

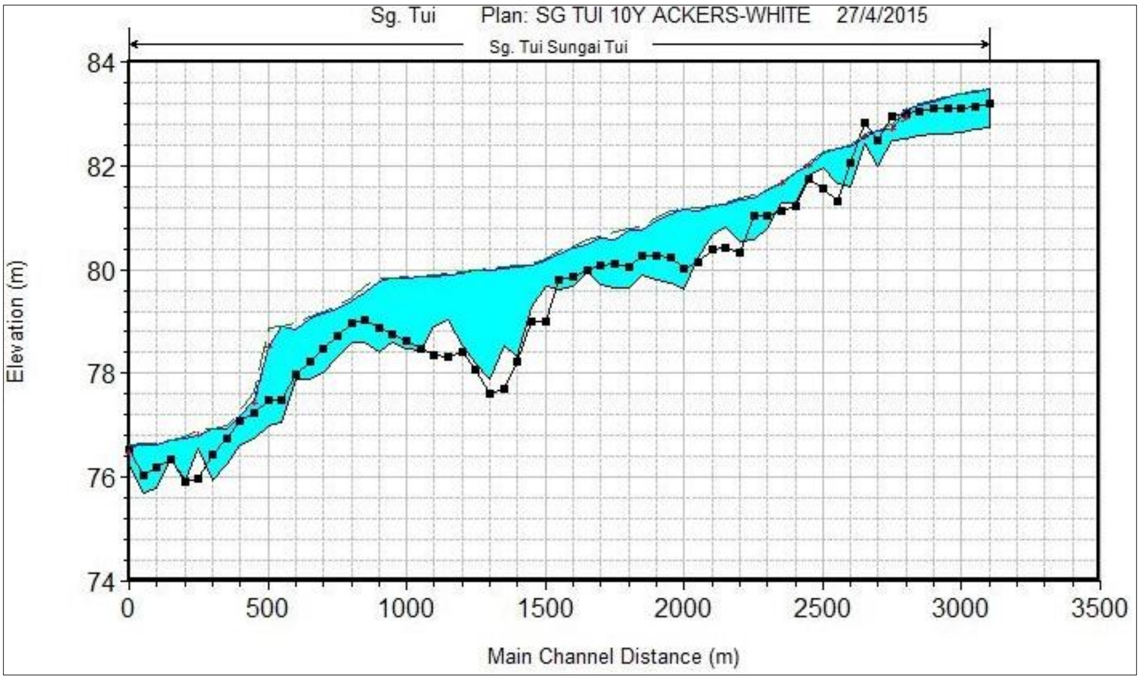

Figure 4.22: Pattern of sediment transport using the method of Ackers-White for 10 years analysis

4.5.2 England-Hansen

The elevation of the bed stream changes from 80.14 m to 80.06 m at the cross section of 2450 (75 m from upstream bridge). Deposition occurs at the depth of 0.08 m. The elevation of the bed stream changes from 80.03 m to 79.55 m at the cross section of 2400 (25 m from upstream bridge). Erosion occurs at the depth of 0.48 m. The elevation of the bed stream changes from 80.23 m to 79.73 m at the cross section of 2350 (25 m from downstream bridge). Erosion occurs at the depth of 0.50 m. The elevation of the bed stream changes from 80.28 m to 79.79 m at the cross section of 2300 (75 m from downstream bridge). Erosion occurs at the depth of 0.49 m.

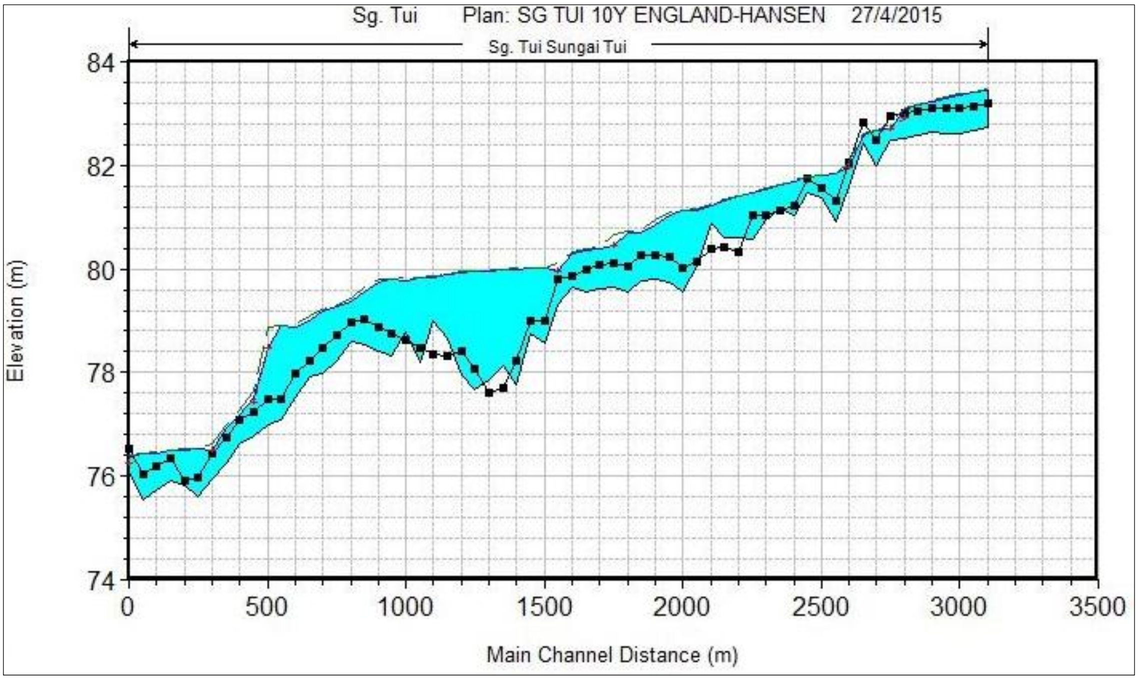

Figure 4.23: Pattern of sediment transport using the method of England-Hansen for 10 years analysis

4.5.3 Laursen

The elevation of the bed stream changes from 80.14 m to 80.32 m at the cross section of 2450 (75 m from upstream bridge). Deposition occurs at the depth of 0.18 m. The elevation of the bed stream changes from 80.03 m to 79.78 m at the cross section of 2400 (25 m from upstream bridge). Erosion occurs at the depth of 0.25 m. The elevation of the bed stream changes from 80.23 m to 79.74 m at the cross section of 2350 (25 m from downstream bridge). Erosion occurs at the depth of 0.49 m. The elevation of the bed stream changes from 80.28 m to 79.79 m at the cross section of 2300 (75 m from downstream bridge). Erosion occurs at the depth of 0.49 m.

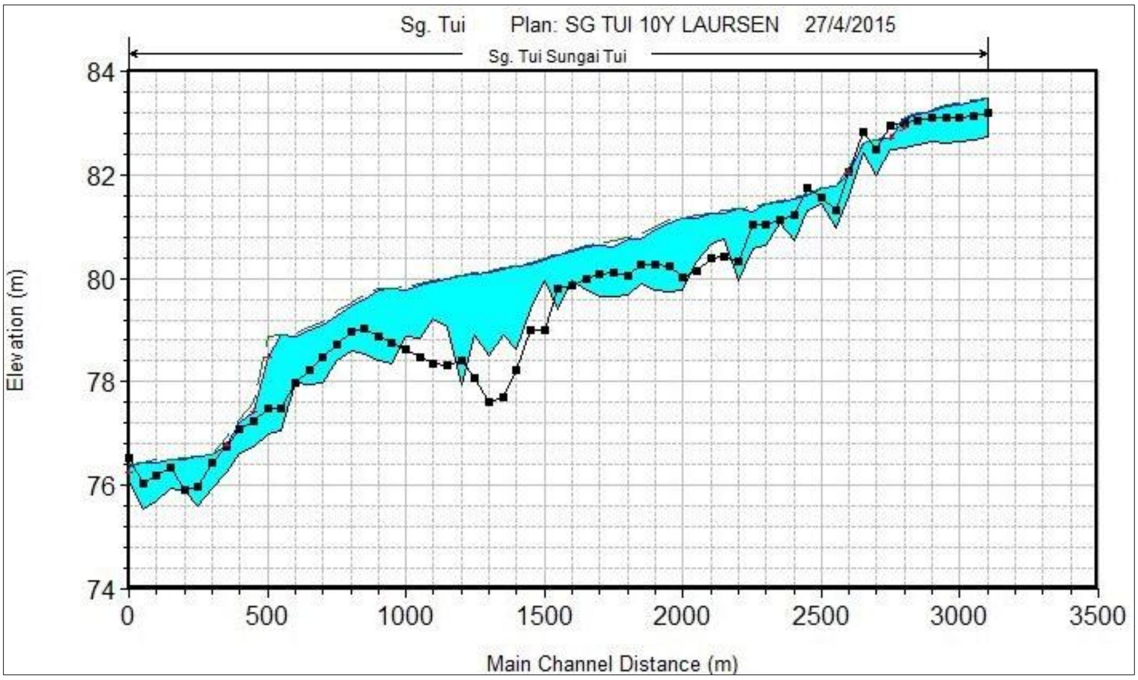

Figure 4.24: Pattern of sediment transport using the method of Laursen for 10 years analysis.

4.5.4 Meyer Peter Muller

The elevation of the bed stream changes from 80.14 m to 80.18 m at the cross section of 2450 (75 m from upstream bridge). Deposition occurs at the depth of 0.04 m. The elevation of the bed stream changes from 80.03 m to 79.55 m at the cross section of 2400 (25 m from upstream bridge). Erosion occurs at the depth of 0.48 m. The elevation of the bed stream changes from 80.23 m to 79.75 m at the cross section of 2350 (25 m from downstream bridge). Erosion occurs at the depth of 0.48 m. The elevation of the bed stream changes from 80.28 m to 79.91 m at the cross section of 2300 (75 m from downstream bridge). Erosion occurs at the depth of 0.37 m.

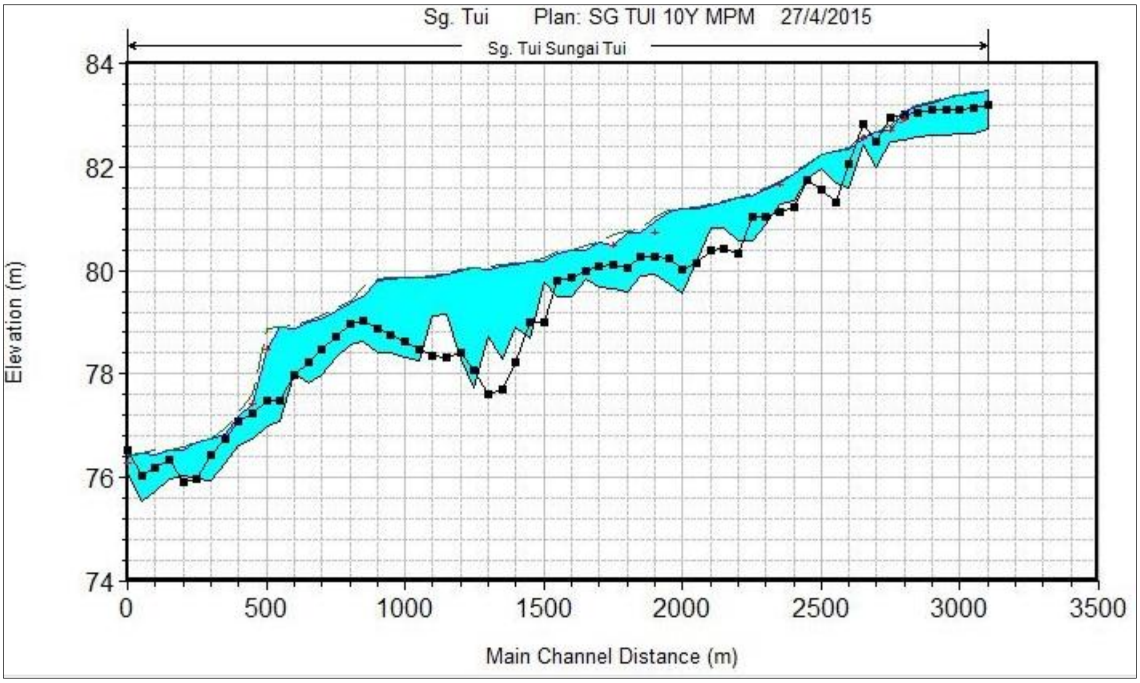

Figure 4.25: Pattern of sediment transport using the method of Meyer Peter Muller for 10 years analysis

4.5.5 Toffaleti

The elevation of the bed stream changes from 80.14 m to 80.01 m at the cross section of 2450 (75 m from upstream bridge). Deposition occurs at the depth of 0.13 m. The elevation of the bed stream changes from 80.03 m to 79.78 m at the cross section of 2400 (25 m from upstream bridge). Erosion occurs at the depth of 0.25 m. The elevation of the bed stream changes from 80.23 m to 79.74 m at the cross section of 2350 (25 m from downstream bridge). Erosion occurs at the depth of 0.49 m. The elevation of the bed stream changes from 80.28 m to 79.79 m at the cross section of 2300 (75 m from downstream bridge). Erosion occurs at the depth of 0.49 m.

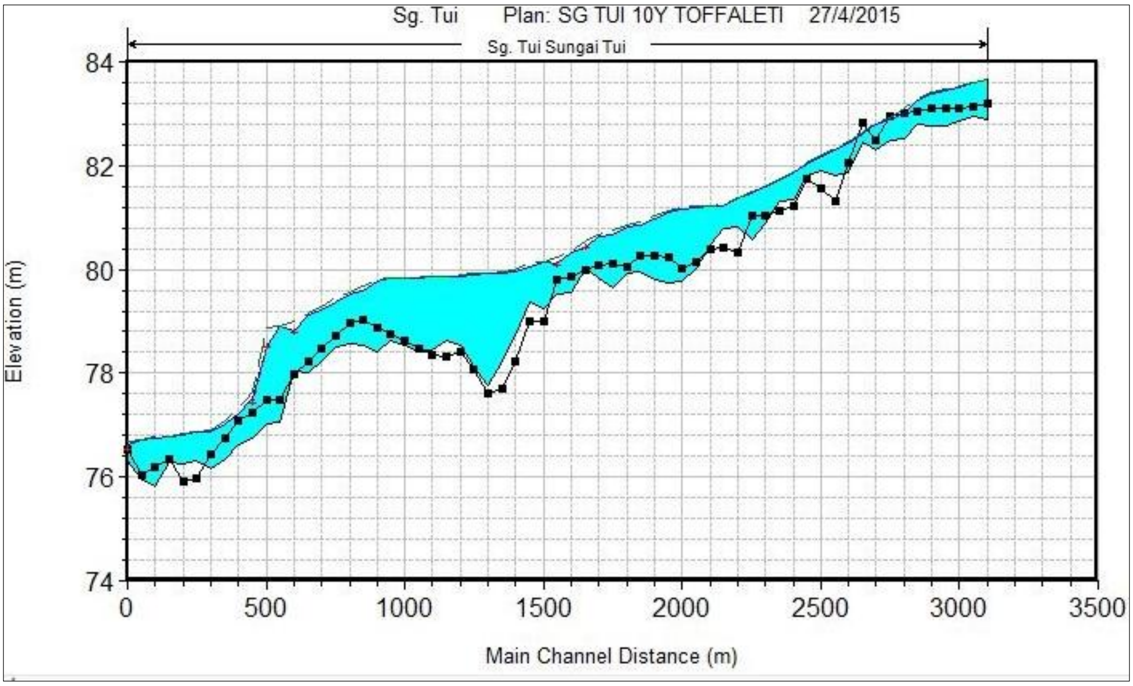

Figure 4.26: Pattern of sediment transport using the method of Toffaleti for 10 years analysis

4.5.6 Wilcock

The elevation of the bed stream changes from 80.14 m to 80.12 m at the cross section of 2450 (75 m from upstream bridge). Erosion occurs at the depth of 0.02 m. The elevation of the bed stream changes from 80.03 m to 79.92 m at the cross section of 2400 (25 m from upstream bridge). Erosion occurs at the depth of 0.11 m. The elevation of the bed stream changes from 80.23 m to 79.83 m at the cross section of 2350 (25 m from downstream bridge). Erosion occurs at the depth of 0.40 m. The elevation of the bed stream changes from 80.28 m to 80.20 m at the cross section of 2300 (75 m from downstream bridge). Erosion occurs at the depth of 0.08 m.

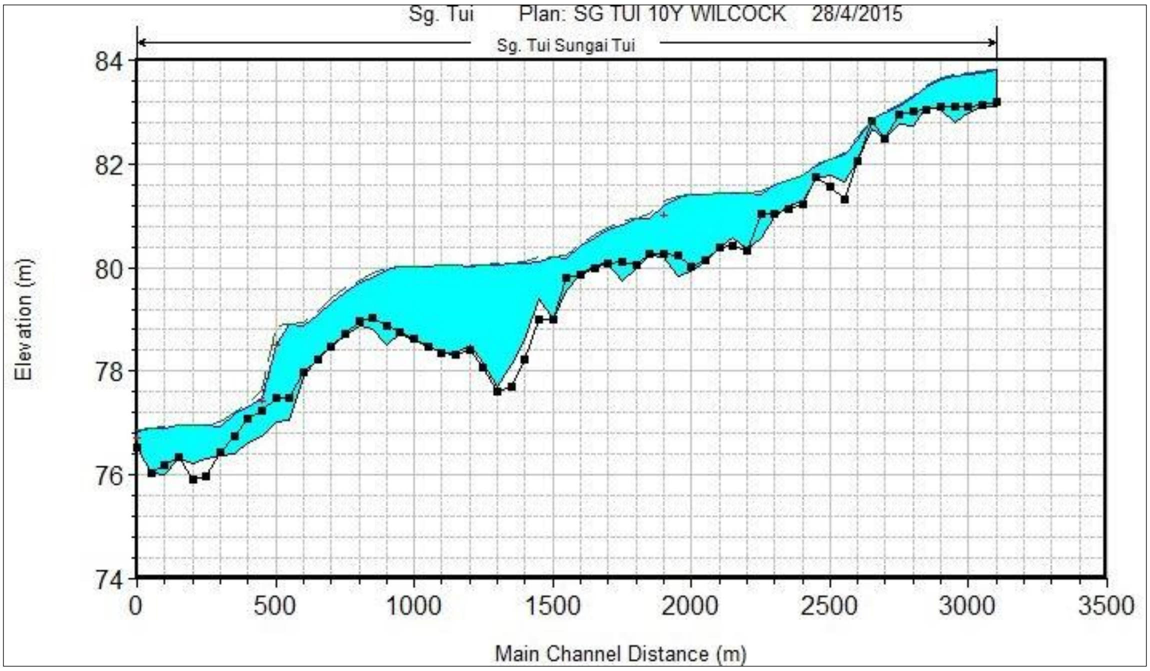

Figure 4.27: Pattern of sediment transport using the method of Wilcock for 10 years analysis

4.5.7 Yang

The elevation of the bed stream changes from 80.14 m to 80.08 m at the cross section of 2450 (75 m from upstream bridge). Deposition occurs at the depth of 0.06 m. The elevation of the bed stream changes from 80.03 m to 79.55 m at the cross section of 2400 (25 m from upstream bridge). Erosion occurs at the depth of 0.48 m. The elevation of the bed stream changes from 80.23 m to 79.75 m at the cross section of 2350 (25 m from downstream bridge). Erosion occurs at the depth of 0.48 m. The elevation of the bed stream changes from 80.28 m to 79.85 m at the cross section of 2300 (75 m from downstream bridge). Erosion occurs at the depth of 0.43 m.

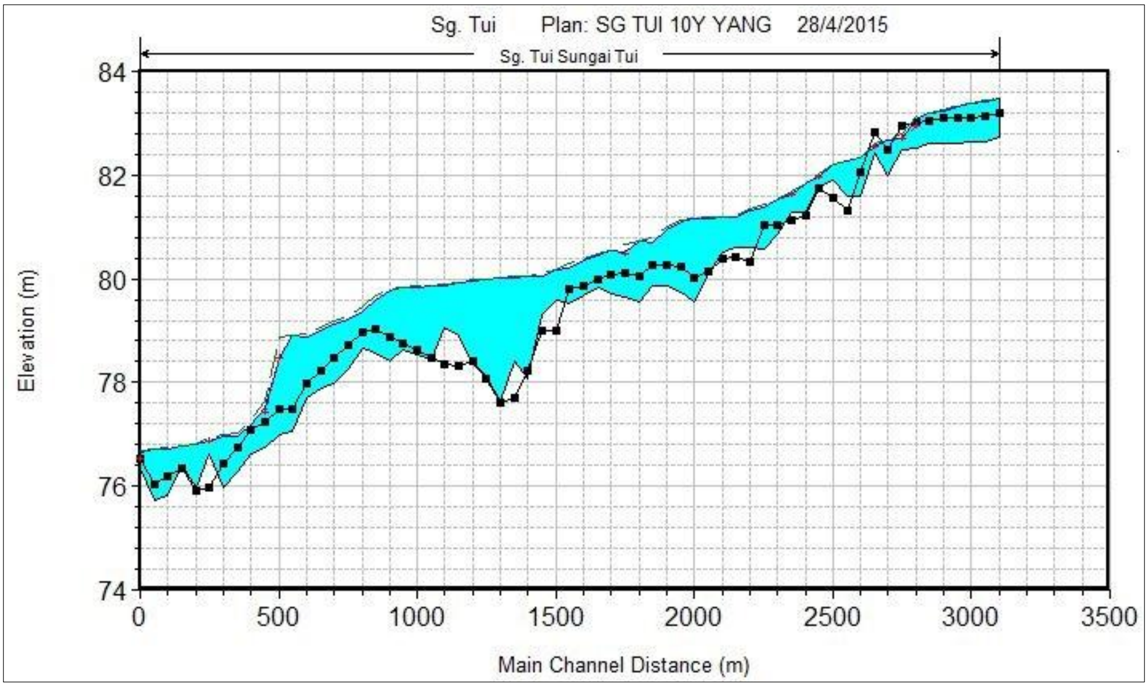

Figure 4.28: Pattern of sediment transport using the method of Yang for 10 years analysis

4.6 COMPARISON BETWEEN METHOD OF TRANSPORT FUNCTIONS

4.6.1 One (1) Year Analysis

The comparison between method of Acker-White, England-Hansen, Laursen, Meyer Peter Muller, Tofaleti, Yang and Wilcock for 1 year sediment transport analysis can be seen in the Table 4.1.

Table 4.1: Comparison between method of transport functions for 1 year analysis

Transport Function	Cross Section	Elevation of stream bed (m)	Elevation of stream bed after sediment transport (m)	Erosion depth (m)	Deposition depth (m)
Acker-White	2450	80.14	80.12	0.02	
	2400	80.03	79.94	0.09	
	2350	80.23	79.81	0.42	
	2300	80.28	79.8	0.48	
England-Hansen	2450	80.14	80.17		0.03
	2400	80.03	79.55	0.48	
	2350	80.23	79.75	0.48	
	2300	80.28	79.79	0.49	
Laursen	2450	80.14	80.34		0.2
	2400	80.03	79.64	0.39	
	2350	80.23	79.74	0.49	
	2300	80.28	79.79	0.49	
Meyer Peter Muller	2450	80.14	80.11	0.03	
	2400	80.03	79.9	0.13	
	2350	80.23	79.74	0.49	
	2300	80.28	79.8	0.48	
Tofaletti	2450	80.14	80.12	0.02	
	2400	80.03	80.01	0.02	
	2350	80.23	79.98	0.25	
	2300	80.28	80.02	0.26	
Yang	2450	80.14	80.11	0.03	
	2400	80.03	79.94	0.09	
	2350	80.23	79.83	0.4	
	2300	80.28	79.85	0.43	
Wilcock	2450	80.14	80.13	0.01	
	2400	80.03	80.02	0.01	
	2350	80.23	80.17	0.06	
	2300	80.28	80.26	0.02	

4.6.2 Three (3) Year Analysis

The comparison between method of Acker-White, England-Hansen, Laursen, Meyer Peter Muller, Tofaleti, Yang and Wilcock for 3 years sediment transport analysis can be seen in the Table 4.2.

Table 4.2: Comparison between method of transport functions for 3 year analysis

Transport Function	Cross Section	Elevation of stream bed (m)	Elevation of stream bed after sediment transport (m)	Erosion depth (m)	Deposition depth (m)
Acker-White	2450	80.14	80.15		0.01
	2400	80.03	79.81	0.22	
	2350	80.23	79.75	0.48	
	2300	80.28	79.8	0.48	
England-Hansen	2450	80.14	80.13	0.01	0.03
	2400	80.03	79.55	0.48	
	2350	80.23	79.74	0.49	
	2300	80.28	79.79	0.49	
Laursen	2450	80.14	80.31		0.17
	2400	80.03	79.88	0.15	
	2350	80.23	79.74	0.49	
	2300	80.28	79.79	0.49	
Meyer peter muller	2450	80.14	80.19		0.05
	2400	80.03	79.72	0.31	
	2350	80.23	79.74	0.49	
	2300	80.28	79.83	0.45	
Tofaletti	2450	80.14	80.1	0.04	
	2400	80.03	79.95	0.08	
	2350	80.23	79.84	0.39	
	2300	80.28	79.9	0.38	
Yang	2450	80.14	80.33		0.19
	2400	80.03	79.77	0.26	
	2350	80.23	79.75	0.48	
	2300	80.28	79.81	0.47	
Wilcock	2450	80.14	80.13	0.01	
	2400	80.03	79.99	0.04	
	2350	80.23	80.08	0.15	
	2300	80.28	80.25	0.03	

4.6.3 Five (5) Year Analysis

The comparison between method of Acker-White, England-Hansen, Laursen, Meyer Peter Muller, Tofaleti, Yang and Wilcock for 5 years sediment transport analysis can be seen in the Table 4.3.

Table 4.3: Comparison between method of transport functions for 5 year analysis

Transport Function	Cross Section	Elevation of stream bed (m)	Elevation of stream bed after sediment transport (m)	Erosion depth (m)	Deposition depth (m)
Acker-White	2450	80.14	80.22		0.08
	2400	80.03	79.72	0.31	
	2350	80.23	79.74	0.49	
	2300	80.28	79.82	0.46	
England-Hansen	2450	80.14	80.11	0.03	
	2400	80.03	79.55	0.48	
	2350	80.23	79.74	0.49	
	2300	80.28	79.79	0.49	
Laursen	2450	80.14	80.3		0.16
	2400	80.03	79.8	0.23	
	2350	80.23	79.74	0.49	
	2300	80.28	79.79	0.49	
Meyer peter muller	2450	80.14	80.27		0.13
	2400	80.03	79.7	0.33	
	2350	80.23	79.74	0.49	
	2300	80.28	79.85	0.43	
Tofaletti	2450	80.14	80.06	0.08	
	2400	80.03	79.9	0.13	
	2350	80.23	79.78	0.45	
	2300	80.28	79.82	0.46	
Yang	2450	80.14	80.19		0.05
	2400	80.03	79.68	0.35	
	2350	80.23	79.75	0.48	
	2300	80.28	79.81	0.47	
Wilcock	2450	80.14	80.13	0.01	
	2400	80.03	79.97	0.06	
	2350	80.23	80	0.23	
	2300	80.28	80.25	0.03	

4.6.4 Ten (10) Year Analysis

The comparison between method of Acker-White, England-Hansen, Laursen, Meyer Peter Muller, Toffaleti, Yang and Wilcock for 10 years sediment transport analysis can be seen in the Table 4.4.

Table 4.4: Comparison between method of transport functions for 10 year analysis

Transport Function	Cross Section	Elevation of stream bed (m)	Elevation of stream bed after sediment transport (m)	Erosion depth (m)	Deposition depth (m)
Acker-White	2450	80.14	80.24		0.1
	2400	80.03	79.6	0.43	
	2350	80.23	79.75	0.48	
	2300	80.28	79.79	0.49	
England-Hansen	2450	80.14	80.06	0.08	
	2400	80.03	79.55	0.48	
	2350	80.23	79.73	0.5	
	2300	80.28	79.79	0.49	
Laursen	2450	80.14	80.32		0.18
	2400	80.03	79.78	0.25	
	2350	80.23	79.74	0.49	
	2300	80.28	79.79	0.49	
Meyer peter muller	2450	80.14	80.18		0.04
	2400	80.03	79.55	0.48	
	2350	80.23	79.75	0.48	
	2300	80.28	79.91	0.37	
Tofaletti	2450	80.14	80.01	0.13	
	2400	80.03	79.78	0.25	
	2350	80.23	79.74	0.49	
	2300	80.28	79.79	0.49	
Yang	2450	80.14	80.08	0.06	0.19
	2400	80.03	79.55	0.48	
	2350	80.23	79.75	0.48	
	2300	80.28	79.85	0.43	
Wilcock	2450	80.14	80.12	0.02	
	2400	80.03	79.92	0.11	
	2350	80.23	79.83	0.4	
	2300	80.28	80.2	0.08	

CHAPTER 5

CONCLUSION AND RECOMMENDATIONS

5.1 CONCLUSION

As a conclusion, the objectives of this research were accomplished through the stimulation and analysis the pattern of sediment transport around bridge at Sungai Tui, Pahang. The sediment pattern can be predicted and analysis using several method in HEC-RAS software. The pattern of sediment transport using Ackers-White, England-Hansen, Laursen, Meyer Peter Muller, Toffaleti, Yang and Wilcock transport functions produce vary result of analysis. Moreover, erosion and deposition of sediment can be evaluated from the sediment analysis. Flow condition is depending on historical data of the year 1999.

For 1 year analysis, at the cross section of 2450 (75 m from upstream bridge) erosion occur at the depth 0.02 m using Ackers-White; 0.03 m using Meyer Peter Muller; 0.02 m using Toffaleti; 0.03 m using Yang; and 0.01 m using Wilcock, whereas deposition occur at the depth 0.03 m using England-Hansen; and 0.20 m using Laursen. At the cross section of 2400 (25 m from upstream bridge) erosion occur at the depth 0.09 m using Ackers-White; 0.48 m using England-Hansen; 0.39 m using Laursen; 0.03 m using Meyer Peter Muller; 0.02 m using Toffaleti; 0.09 m using Yang; and 0.01 m using Wilcock, whereas no deposition occur. At the cross section of 2350 (25 m from downstream bridge) erosion occur at the depth 0.42 m using Ackers-White; 0.48 m using England-Hansen; 0.49 m using Laursen; 0.49 m using Meyer Peter Muller; 0.25 m using Toffaleti; 0.40 m using Yang; and 0.06 m using Wilcock, whereas no deposition occur. At the cross section of 2300 (75 m from downstream bridge) erosion occur at the depth 0.48m using Ackers-White; 0.49 m using England-Hansen; 0.49 m using Laursen; 0.48 m using Meyer Peter Muller; 0.26 m using Toffaleti; and 0.02 m using Wilcock, whereas deposition occur at the depth 0.03 m using Yang.

For 3 years analysis, at the cross section of 2450 (75 m from upstream bridge) erosion occur at the depth 0.01 m using England-Hansen; and 0.01 m using Wilcock, whereas deposition occur at the depth 0.01 m using Ackers-White; 0.17 m using Laursen; 0.19 m using Meyer Peter Muller; 0.04 m using Toffaleti and 0.19 m using Yang. At the cross section of 2400 (25 m from upstream bridge) erosion occur at the depth 0.22 m using Ackers-White; 0.48 m using England-Hansen; 0.15 m using Laursen; 0.26 m using Meyer Peter Muller; 0.08 m using Toffaleti 0.26 m using Yang; and 0.04 m using Wilcock, whereas no deposition occur. At the cross section of 2350 (25 m from downstream bridge) erosion occur at the depth 0.48 m using Ackers-White; 0.49 m using England-Hansen; 0.49 m using Laursen; 0.48 m using Meyer Peter Muller; 0.39 m using Toffaleti 0.48 m using Yang; and 0.15 m using Wilcock, whereas no deposition occur. At the cross section of 2300 (75 m from downstream bridge) erosion occur at the depth 0.48m using Ackers-White; 0.49 m using England-Hansen; 0.49m using Laursen; 0.47 m using Meyer Peter Muller; 0.38 m using Toffaleti 0.47 m using Yang; and 0.03 m using Wilcock, whereas no deposition occur.

For 5 year analysis, at the cross section of 2450 (75 m from upstream bridge) erosion occur at the depth 0.03 m using England-Hansen; 0.08 m using Toffaleti; and 0.01 m using Wilcock, whereas deposition occur at the depth 0.08 m using Ackers-White; 0.16 m using Laursen; 0.13 m using Meyer Peter Muller; and 0.05 m using Yang. At the cross section of 2400 (25 m from upstream bridge) erosion occur at the depth 0.31 m using Ackers-White; 0.48 m using England-Hansen; 0.23 m using Laursen; 0.33 m using Meyer Peter Muller; 0.13 m using Toffaleti 0.35 m using Yang; and 0.06 m using Wilcock, whereas no deposition occur. At the cross section of 2350 (25 m from downstream bridge) erosion occur at the depth 0.49 m using Ackers-White; 0.49 m using England-Hansen; 0.49 m using Laursen; 0.49 m using Meyer Peter Muller; 0.45 m using Toffaleti 0.48 m using Yang; and 0.23 m using Wilcock, whereas no deposition occur. At the cross section of 2300 (75 m from downstream bridge) erosion occur at the depth 0.46 m using Ackers-White; 0.49 m using England-Hansen;

0.49 m using Laursen; 0.43 m using Meyer Peter Muller; 0.46 m using Toffaleti 0.47 m using Yang; and 0.03 m using Wilcock, whereas no deposition occur.

For 10 year analysis, at the cross section of 2450 (75 m from upstream bridge) erosion occur at the depth 0.08 m using England-Hansen; 0.13 m using Toffaleti; 0.06 m using Yang; and 0.02 m using Wilcock, whereas deposition occur at the depth 0.10 m using Ackers-White; 0.18 m using Laursen; and 0.04 m using Meyer Peter Muller. At the cross section of 2400 (25 m from upstream bridge) erosion occur at the depth 0.43 m using Ackers-White; 0.48 m using England-Hansen; 0.25 m using Laursen; 0.48 m using Meyer Peter Muller; 0.25 m using Toffaleti 0.48 m using Yang; and 0.11 m using Wilcock, whereas no deposition occur. At the cross section of 2350 (25 m from downstream bridge) erosion occur at the depth 0.48 m using Ackers-White; 0.50 m using England-Hansen; 0.49 m using Laursen; 0.48 m using Meyer Peter Muller; 0.49 m using Toffaleti 0.48 m using Yang; and 0.40 m using Wilcock, whereas no deposition occur. At the cross section of 2300 (75 m from downstream bridge) erosion occur at the depth 0.48 m using Ackers-White; 0.49 m using England-Hansen; 0.49 m using Laursen; 0.37 m using Meyer Peter Muller; 0.49 m using Toffaleti 0.43 m using Yang; and 0.08 m using Wilcock, whereas no deposition occur.

5.2 RECOMMENDATIONS

In forthcoming, it is recommended that, more research should carry out in sedimentation as the key to understand the fundamental sedimentation process and principles comprehend. The damages create by sediment are wide-ranging depend on the amount of sediment is influenced by the process of erosion, transport and deposition. Significant knowledge is desirable comparative to the different aspects of erosion, transport and deposition of sediment before accurate foresights of causes and effects can be determined.

Historical data for river bed in to select the appropriate approach for sediment transport. HEC HMS is capable to stimulate the rainfall-runoff processes of watershed. The software generates hydrograph directly or in coincides with other software for knowledge of flow forecasting, urban drainage, future development, systems operation, flood damage reduction, floodplain regulation, water availability and basin spillway design. HEC RAS is leading software designed for one-dimensional hydraulic analysis. The software consists of four elements for steady flow water surface calculation, unsteady flow stimulation, water quality analysis, and sediment transport stimulation that use hydraulic computation routines and geometric data. Basic water surface profiles can generate using several hydraulic design features. In addition, HEC RAS can predict the changes in channel bed and river profiles from troubles such as floodplain.

REFERENCES

Ackers, P. and White, W.R. 1973. Sediment transport: new approach and analysis. *Journal of the Hydmulics Division ASCE*. **99**: 2041 -2060.

Allen, J.R.L. 1965. A review of the origin and characteristics of recent alluvial sediments. *Sedimentology*. **5**: 89-191.

Ashley, G.M. 1990. A unifying classification scheme for environmental discriminators; Large-scale flow-transverse subaqueous bedforms. *International Sedimentological Congress*. **13:** 11–12.

Bennett, H.H. 1939. *Soil conservation*. New York: McGraw-Hill Book Co Inc.

Brune, G.M. 1958. Sediment is Your Problem. Agricultural Information Bulletin No. 174, Soil Conservation Service, March.

Craven, J.P. 1953. The transportation of sand in pipes. *Proceedings of the 5th Hydraulic Conference*. **3**4: 67-76

Dyer, K.R. and Soulsby, R. L. 1988. *Fluid Mechanics.* **20: 295–324**. USA: Annual Reviews.

Einstein, H.A. 1942. Formulas for the transportation of bed load. *Transactions ASCE* **107**: 561-573

Ellis. M. M. 1936. Erosion silt as afactor in aquatic environments. Ecology 17: 29-42.

Engelund, F. and Hansen, E. 1972. A Monograph on Sediment Transport in Alluvial Streams. Teknisk Forlag, Copenhagen, Denmark.

Gregory, K.J. 1977. *River Channel Changes*, New York: Wiley-Interscience.

Gurnell, A. and Petts, G. Eds. 1995. *Changing River Channels*. Chichester: John Wiley and Sons.

Hayter, E.J. 1983. *Prediction of cohesive sediment movement in estuarial waters*. Ph.D. Thesis, the University of Florida at Gainesville, USA.

Horton, R.E. 1932. *Drainage Basin Characteristics*. Trans AGU. **13**: 350–361.

Jansen, P., Van Bendegom L., Van den Berg J., Vries M.den. and Zanen, A. 1979. *Principles of River Engineering: The Non-Tidal Alluvial River,* San Francisco: Pitman.

Julien P.Y. 2002. *River mechanics*. New York: Cambridge University Press

Laursen, E.M. 1956. The hydraulics of a storm drain system for sediment transporting flow. *Iowa Highwayway Research Board.*. **84**: 1530-36.

Laursen, E.M. 1958. The Total Sediment Load of Streams. *Journal of the Hydraulics Division ASCE*. **84**: 1530-36.

Leopold, L.B. and Wolman, M.G. 1964. *River Meanders*. Geol. Soc. of Am., Bull., No. **71**: 769-794.

Lewin, J. 1977. Channel pattern changes. *In River Channel Changes*. USA: John Wiley and Sons. **8**: 167-184

McLean, S.R. 1992. On the calculation of suspended load for noncohesive sediments *Journal of Geophysical Research*. AGU, **97**: 5759-5770.

Meyer-Peter, E. and Muller R. 1948. Formulas for Bedload Transport, *Proceedings, the Second Meeting of the International Association for Hydraulic Structures Research*, Stockholm.

Newson, M.D. 1995. Fluvial geomorphology and environmental design. *In Changing River Channels*. USA: John Wiley and Sons. **19:** 413-432

Rouse, H., 1937. Modern conceptions of the mechanics of fluid turbulence. Trans. A.S.C.E., 102, 463-543.

Rysgaard, S., P.B. Christensen and L.P. Nielsen. 1995. *Seasonal variation in nitrification and denitrifiction in estuarine sediment colonized by benthic microalgae and bioturbating infauna*. Mar. Ecol. Prog. Ser. **126**:111-121.

Schumm, S.A. 1969. River metamorphosis. *Journal of the Hydraulics Division ASCE*. **95**: 255-273.

Schumm, S.A. 1971. Fluvial Geomorphology. *In River Mechanics*. **5**. Fort Collins, USA: Ed. Shen H.W.

Schumm, S. A., 1977, *The Fluvial System*, Wiley, New York.

Simons, daryl B. and Sentruk Fuat. 1992. *Sediment Transport Technology*. Littleton Colorado: Water Resurces Publication.

Stephens, K.P., Lavoie, D.L., Briggs, K.B., Furukawa, Y. and Richardson, M.D. 1997. Geotechnical and Geoacoustic Properties of Sediments off South Florida: Boca Raton, Indian Rocks Beach, Lower Tampa Bay, and the Lower Florida Keys. Report NRL/MR/7431--97-8042, Naval Research Laboratory: Stennis Space Center. pp. 310.

Toffaleti, F.B. 1969. Definitive Computations of Sand Discharge in Rivers. *Journal of the Hydraulics Division ASCE.* **95**: 225-246.

U.S. Army Corps of Engineers. 1995. River analysis system. HEC-RAS User's Manual Version 1.0. Hydrologic Engineering Center, Davis, CA.

Van Leussen W. 1994. *Estuarine macroflocs and their role in fine-grained sediment transport*. PhD thesis, Universiteit Utrecht, 488 pp.

Van Rijn, L.C. 1984. Sediment transport, part II, suspended load transport. *Journal of the Hydraulic Division ASCE*. **110: 1613–1641.**

Vanoni, V.A., 1946. Transportation of suspended sediment by water. Trans. A.S.C.E., 111: 67-133.

Vanoni, V.A. ed. 1977. *Sedimentation Engineering, Manuals and Reports on Engineering*. New York: American Society of Civil Engineers..

Wang, G.Q. and Ni, J.R. 1991. The kinetic theory for dilute solid/liquid two-phase flow. Int. J. Multiphase Flow, **17:** 273–281.

Wilcock, P.R. and Crowe, J.C. 2003. Surface-based transport model for mixed-size sediment. *Journal of Hydraulic Engineering*. **129(2)**: 120-128.

Yang, C.T. 1972. Unit Stream Power and Sediment Transport. *Journal of the Hydraulic Division ASCE.* **18:** 1805- 1 826.